2006

Opto-Electronic Processes in SrS:Cu ACTFEL Devices

Dharmashankar Rajagopalan
University of Kentucky, draja2@uky.edu

ABSTRACT OF THESIS

Opto-Electronic Processes in SrS:Cu ACTFEL Devices

The a. c. thin film electroluminescent (ACTFEL) devices are of scientific interest due to their applications in large area, flat panel displays. Of particular interest to the research community is the mechanism of electron transport and luminance in these devices. Toward this end, a physical model and a mathematical model for SrS:Cu ACTFEL Devices were developed and published earlier by our group. The purpose of this thesis is to obtain a qualitative and quantitative match between experiment and theory. A brief summary of the model can be found here [1]. Effects of variation in drive parameters in experimental steady state measurements, and analysis of VIL (Voltage-Current-Luminance) plots for different simulated device and drive parameters are performed. The effects of voltage amplitude, activator concentration, interface energy levels, and critical field for dipole collapse were studied.

The plots matched qualitatively in that all major experimental features were produced in the simulated waveforms. The measured and the simulated peak currents are 72.5 mA/cm^2 and 66.42 mA/cm^2 for V_A = 123 V. Experimental and theoretical charge transferred per pulse were 2.75 $\mu C/cm^2$ and 2.26 $\mu C/cm^2$. Peak experimental and simulated luminance values for V_A = 123 V were 531 cd/m^2 and 49150 cd/m^2. Total experimental and simulated luminance values for V_A = 123 V case were 6.2 cd/m^2 and 561.2 cd/m^2 respectively. The large difference is attributed to the loss factors such as optical losses (due to total internal reflection), scattering of electrons by impurities in the bulk phosphor layer, and concentration quenching; these have not been incorporated in the model yet.

KEY WORDS: ACTFEL, Electroluminescent Displays, Flat Panel Displays, Phosphors, SrS

_____

_____

Opto-Electronic Processes in SrS:Cu ACTFEL Devices

By

Dharmashankar Rajagopalan

_____
Director of Thesis

_____
Director of Graduate Studies

_____

RULES FOR THE USE OF THESES

Unpublished thesis submitted for the Master's degree and deposited in the University of Kentucky Library are as a rule open for inspection, but are to be used only with due regard to the rights of the authors. Bibliographical references may be noted, but quotations or summaries of parts may be published only with the permission of the author, and with the usual scholarly acknowledgments.

Extensive copying or publication of the dissertation in whole or in part also requires the consent of the Dean of the Graduate School of the University of Kentucky.

A library that borrows this dissertation for use by its patrons is expected to secure the signature of each user.

Name Date

THESIS

Dharmashankar Rajagopalan

The Graduate School

University Of Kentucky

2006

Opto-Electronic Processes in SrS:Cu ACTFEL Devices

THESIS

A thesis submitted in partial fulfillment of the
requirements for the degree of Master of Science in the
College of Engineering
at the University of Kentucky

By

Dharmashankar Rajagopalan

Director: Dr. Vijay Singh, Department of Electrical Engineering

Lexington, Kentucky

2006

MASTER'S THESIS RELEASE

I authorize the University of Kentucky
Libraries to reproduce this thesis in
whole or in part for purposes of research.

Signed: _____

Date: _____

DEDICATION

To all my family members and friends.

ACKNOWLEDGEMENTS

This leaf signifies a simple but earnest attempt by me to acknowledge the "behind the scenes" role enacted, in successfully completing my Master's thesis. To start off, my profound thanks to **Dr. Vijay Singh**, Chairman who has been the impetus and source of inspiration in my project work.

I am obligated to **Dr. Alberto Aguilera** for his valuable and opportune suggestions that kept me going when the going got tough. I extend my gracious thanks to **Mr. Praveen Sivakumar** whose contribution is irrefutably the most staple of all. My heartfelt thanks to **Mr. Vignesh Ramachandran**, and **Mrs. Karen Sampson** for their assistance while taking measurements.

I would like to thank Dr. Vijay Singh, Dr. Janet Lumpp and Dr. Ingrid St. Omer for serving on my committee. I would like to thank my family for their support and encouragement.

This work was supported in part by a grant from Batelle Inc (02143). Thanks are due to Planar America for supplying some of the devices used for this study and to Dr. Chris King and Dick Tuengue for fruitful comments and discussions.

TABLE OF CONTENTS

List of Figures

List of Files

DRThes.pdf……...……...…2.20 MB

Chapter 1

Introduction

A display, is this context, is an electronic component or subsystem used to convert electrical signals into visual image. The computer terminal using a cathode ray tube (CRT) or flat panel is one of the most important industrial applications of electronic displays. The electronic displays are also used for presentations of graphs, symbols, and video pictures. It is believed that because of substantial reduction in size, weight and power, flat panel displays (FPD) will replace more and more CRT displays in the near future. At present the four major technologies for FPD are:

- Liquid crystal displays (LCD)
- Plasma displays (PD)
- Field emission displays (FED)
- Electroluminescent displays

Electroluminescent devices are solid state devices, have fast response, wide viewing angle, high resolution, wide operating temperatures and all are light weight. They have generated great scientific as well as commercial interest.

Electroluminescent displays are based on the phenomenon of luminescence, which is non thermal radiation of optical energy when an electron makes a radioactive transition from a higher to a lower energy level. The two types of electroluminescence are:

- Injection electroluminescence
- High field electroluminescence.

In high field electroluminescence, the electrical energy is supplied by high field (in the order of 10^8 V/m), which accelerates electrons in a host material to very high velocities.

Electroluminescence refers to non-thermal generation of light resulting from the application of an electric field to a substance. EL devices are divided into four types: ac thin film EL, ac powder EL, dc thin-film EL and dc powder EL. Among these, two types are now commercially available: ac thin film EL devices (ZnS:Mn) are used as flat screens of laptop personal computers and word processors, and ac powder EL devices are used as backlights for liquid crystal displays.

In particular, thin film EL devices are preferred because they have the largest possibility to be commercialized widely. They are solid emissive display devices with the following superior characteristics: fast response, wide viewing angles, high resolution wide operating temperatures, light weight, and good display qualities. Thin film EL is also found in applications where good contrast must be maintained in a very high ambient illumination environment such as in industrial instrumentation. The strongest selling point of thin film EL display is high legibility because light is emitted from a sub-micrometer thick device with crisp pixel edges.

The biggest challenge today for the thin-film EL technology is producing multicolor displays. Manufacturing of practical multicolor displays was long delayed due to insufficient luminance of the primary colors. Recently, however progress in the

development of the multicolor display structure and color phosphors have made it possible to fabricate the first multicolor thin-film EL displays. Thin film EL displays can be made with a very simple device structure. The first multicolor thin-film EL displays are based on the inverted patterned-color-filtered device structure, where red and green colors are filtered out from yellow-emitting ZnS:Mn.

Motivation

The purpose of this thesis is to contribute to the understanding of SrS- based ACTFEL devices operation. Using the analytical model for SrS:Cu,Ag A.C. Thin Film Electroluminescent Display Devices the effects of variation in device and drive parameters in Experimental Steady State and Transient measurements were performed. Simulated current and luminance were obtained and were compared with experimental data. These plots were then quantitatively compared and the results of the comparison were presented. Time Resolved Spectroscopy was performed to determine luminescence lifetimes and possible decay mechanisms. Experimental Steady State measurements were performed at different temperatures using Cryostat and the results were analyzed.

Organization of the Thesis

Experimental and simulated procedure is described in Chapter. II. A brief summary of the model is described in Chapter. III. Simulated field; current and luminance are presented in Chapter. IV and compared with experimental data. Effects of variation in device and drive parameters in experimental steady state measurements are described in Chapter. V.

Chapter 2

Experimental Procedure

Display Testing System

The display testing system was developed to test ACTFEL devices for display panel applications and record acquired data for further analysis. Present system allows testing devices in AC mode and recording four different waveform parameters: Applied Voltage, Current through the device, Light Output Response and Charge flowing through the Device. The system is configured to capture one data point every microsecond. The maximum possible voltage is in the range ±500 V, but for available ACTFEL devices, ±160 V is typically used.

System Hardware

The schematic representation of the display system is shown below. A computer running the Display Testing System Software Version 1.0 under LABVIEW 6 controls the system. The computer has GPIB interface card connected through the GPIB bus to the oscilloscope, signal waveform generator and monochromator. The oscilloscope can record four channels

- Applied Voltage to the Device
- Voltage on the Sense Capacitor
- Output of the Photo Multiplier Tube
- Current Output.

The maximum output signal of the waveform generator is 10V. In order to bring the output to the voltage required for device operation, a custom amplifier was built based on the Apex PA89 operational amplifier. Two power supplies connected in series as Master Slave configuration are used to supply power to the built amplifier. The range of sensitivity of the photo multiplier tube was 185-900nm.

Display Testing System Hardware

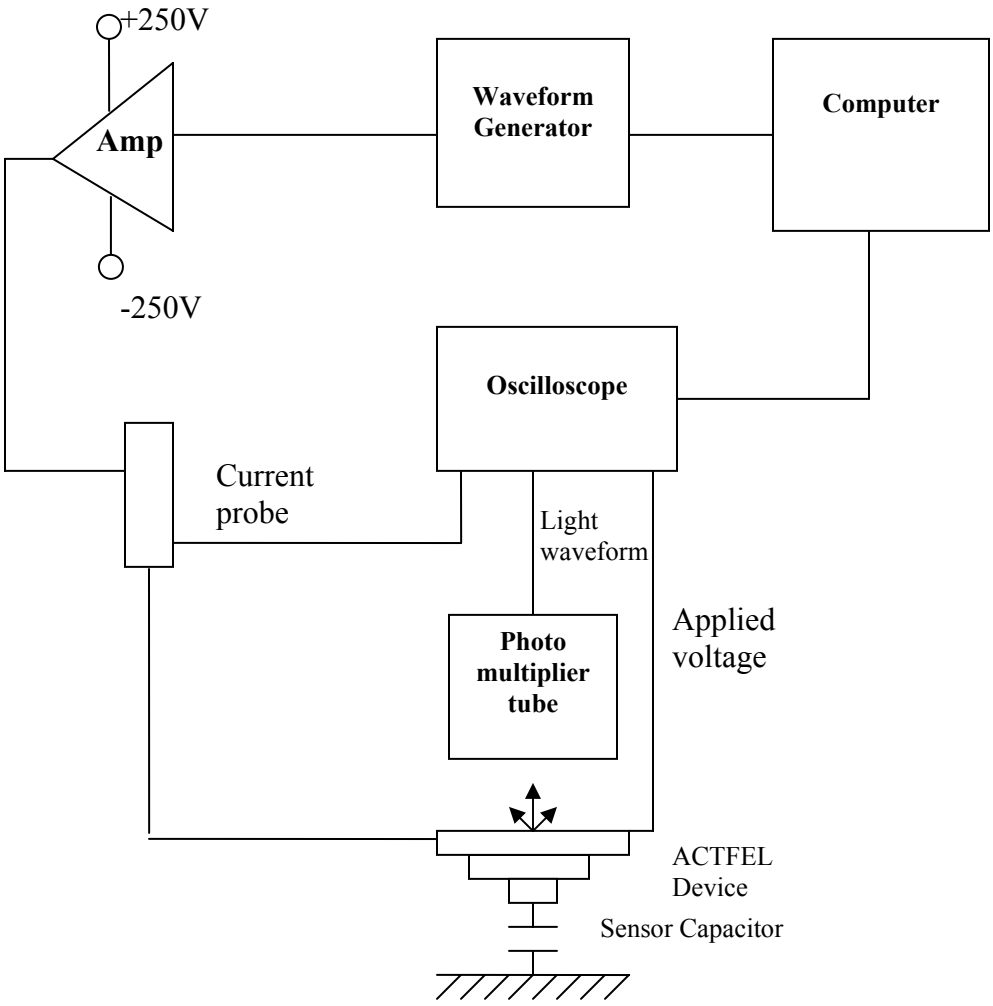

Figure 2.0.1: Block diagram of Display testing System Hardware

Displays Testing System Software

The Display Testing System software was written in Labview 6.0 graphical programming environment. There are three main modes of operation

- Single Measurement (Constants page)
- Excitation Voltage Sweep Mode (Voltage Sweep Page)
- Wavelength sweep Mode (Wavelength Sweep Page)

Constants Page

The parameters that affect all modes of operation are found in the constants page. The parameters that define the pulse are in the middle of the constants page. The Rise time, On time and Fall time determine the shape of the pulse. The Notch Start Time, Notch Length and Notch Depth are all adjustable in the Constants tab. The additional settings in the constant page are the Initial Transient, Leave Output On, and Points to Capture. The Number of Averages setting on the Oscilloscope determines the number of times the waveform is captured and averaged together. Higher averaging reduces noise, but increases the time required for the experiment to complete.

Voltage Sweep Page

In the Voltage Sweep Mode, the waveforms are captured multiple times while the amplitude of the excitation waveform is varied in equal steps.

Wavelength Sweep Page

In this mode, the Monochromator is connected and is turned on. The Monochromator is adjusted and two sets of waveform are recorded. The first waveform set is taken while the device is excited at a voltage low enough so that no luminance is produced. The number of wavelengths produced is determined by the Number of Steps control. The design system is very powerful and flexible tool for experimental measurements.

Simulation Procedure

A mathematical model of the Electroluminescence in SrS:Cu ACTFEL device was developed by Dr.Singh et al ([2]) and in order to verify the model a C program was written in order to verify the validity of the model. The c program incorporated the various mathematical equations that described the method of luminance in SrS:Cu ACTFEL device.

The results of the program were compared with the experimental results obtained & the accurateness of the mathematical model was verified. For the purpose of simulation a trapezoidal applied voltage similar to the one used for experiments was used. The bulk phosphor was divided into “n” smaller sections and the electric field was calculated for each section. The electric flux in each section was taken as the sum of a cumulative sum of fluxes in previous sections and proportional to the electric field calculated in that section. For every instance the cathodic flux and the anodic flux were compared and depending on the magnitude of these fluxes the direction of electron flow was

determined. Here instance refers to a time frame of 50 nanoseconds where it is assumed no significant changes in the electric field or electric flux takes place. Based on the flux the electron population at every energy level was calculated and updated for every instance. The flux in the "n^{th}" was used to calculate the electron population at the shallow interface states. The flow of electrons from a higher energy level to a lower energy level was dependent on the relaxation time.

The whole process was repeated for every 50ns until the total time matched the time period of the trapezoidal applied voltage pulse. In this way the simulation was run for 200 pulses in order to check the validity of the code.

Simulation Procedure and System Flowchart

In order to numerically solve the equations described in [2], a program was coded in C and run in a UNIX environment. The results were then compared with experimentally obtained data. For the purpose of simulation, the phosphor layer was divided into 100 sections. The simulation time increment Δt was chosen to be 50 ns. This choice of Δt was made after varying Δt over a wide range and studying the effects on the results of the simulation. Field and charge in each section were then assumed to be constant over this small time interval Δt and all the processes of interest were calculated based on this assumption. Transition rates were computed during each interval and the space charge, field and current were updated every 50 ns. The simulation procedure is illustrated in the flowchart in Fig. 2.0.2.

As shown in the flowchart above, the data files (in which the simulated voltage, current and luminance curves were stored) were opened. Initial state conditions were set before simulation was actually run. The voltage was "built" according to the required amplitude and rise and fall times and the resultant electric field was calculated in every section. This electric field caused the electrons to tunnel out of the interface states. The resultant population at the interface was updated to reflect this change. The electrons thus ejected from the interfaces caused optoelectronic processes described in the model. When these electrons reach the other end, they were trapped at the other interface and relax from the shallow interface state to the deep interface state subsequently.

Due to the optoelectronic processes taking place in the bulk of the phosphor, the electron densities at the lower and higher energy levels as well as the trap and conduction band density vary and it is calculated as per the equations described in Ref. [2]. Thus, the flux generated at every section adds to the flux ejected from the interface or the previous section. As a result of the activator relaxation luminance is produced in the device and the radiance produced is calculated using the equation described in [1].

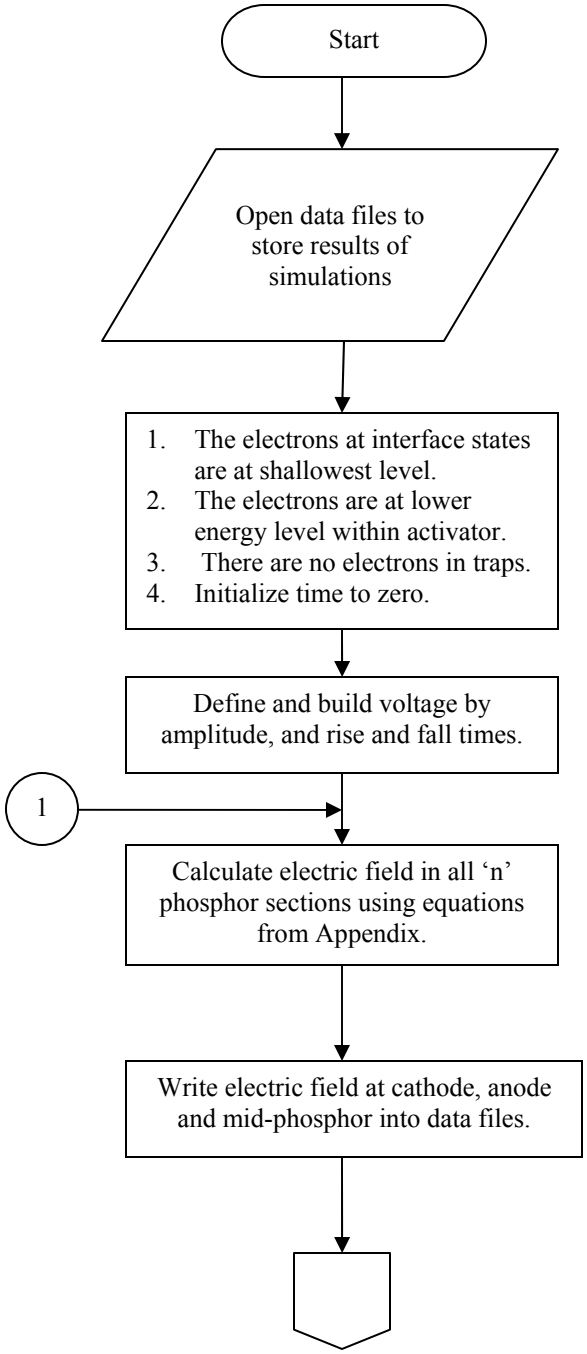
Start
Open data files to store results of simulations
1. The electrons at interface states are at shallowest level.
2. The electrons are at lower energy level within activator.
3. There are no electrons in traps.
4. Initialize time to zero.
Define and build voltage by amplitude, and rise and fall times.
1
Calculate electric field in all ‘n’ phosphor sections using equations from Appendix.
Write electric field at cathode, anode and mid-phosphor into data files.

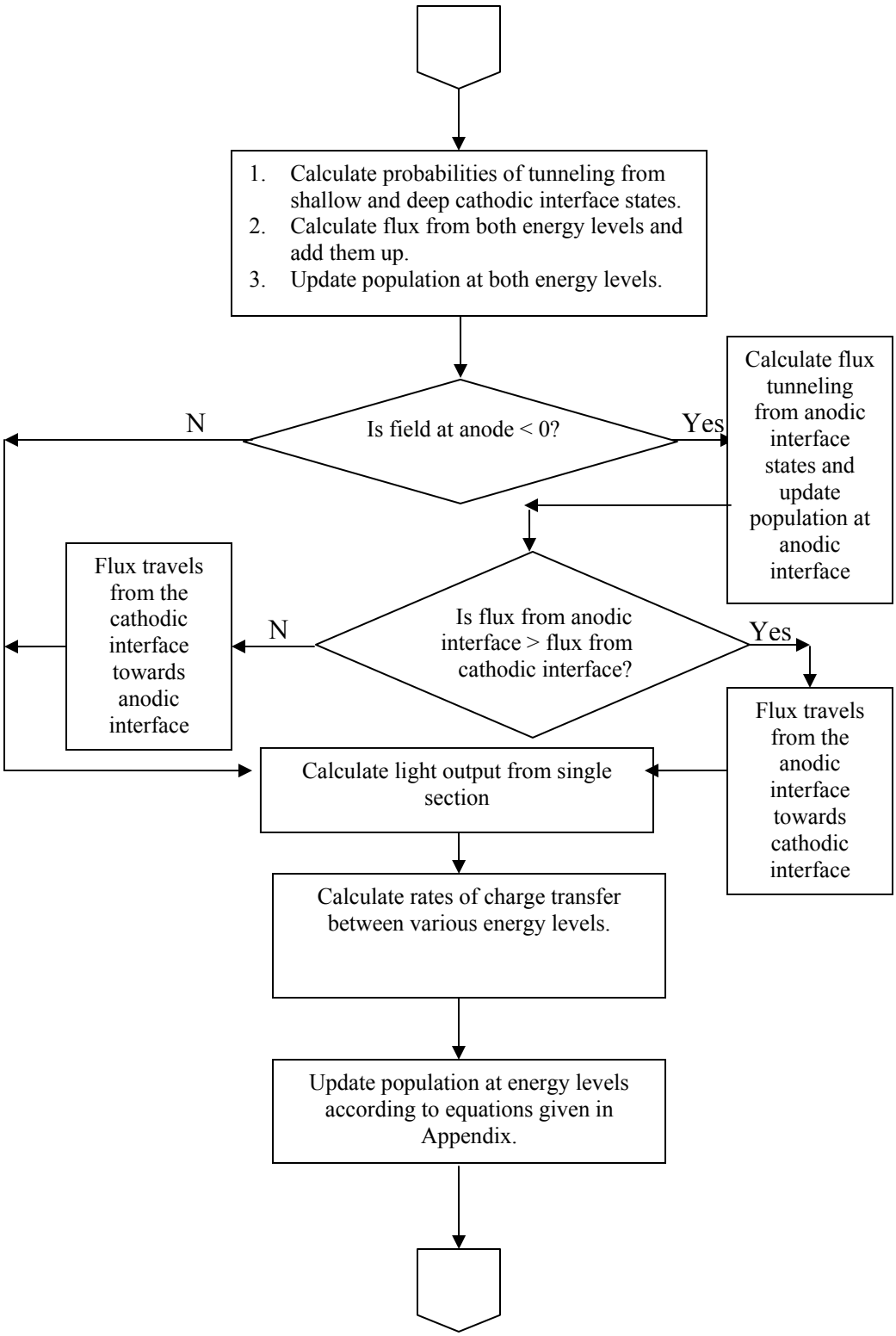
1. Calculate probabilities of tunneling from shallow and deep cathodic interface states.
2. Calculate flux from both energy levels and add them up.
3. Update population at both energy levels.
Is field at anode < 0?
N
Yes
Calculate flux tunneling from anodic interface states and update population at anodic interface
Is flux from anodic interface > flux from cathodic interface?
N
Yes
Flux travels from the cathodic interface towards anodic interface
Flux travels from the anodic interface towards cathodic interface
Calculate light output from single section
Calculate rates of charge transfer between various energy levels.
Update population at energy levels according to equations given in Appendix.

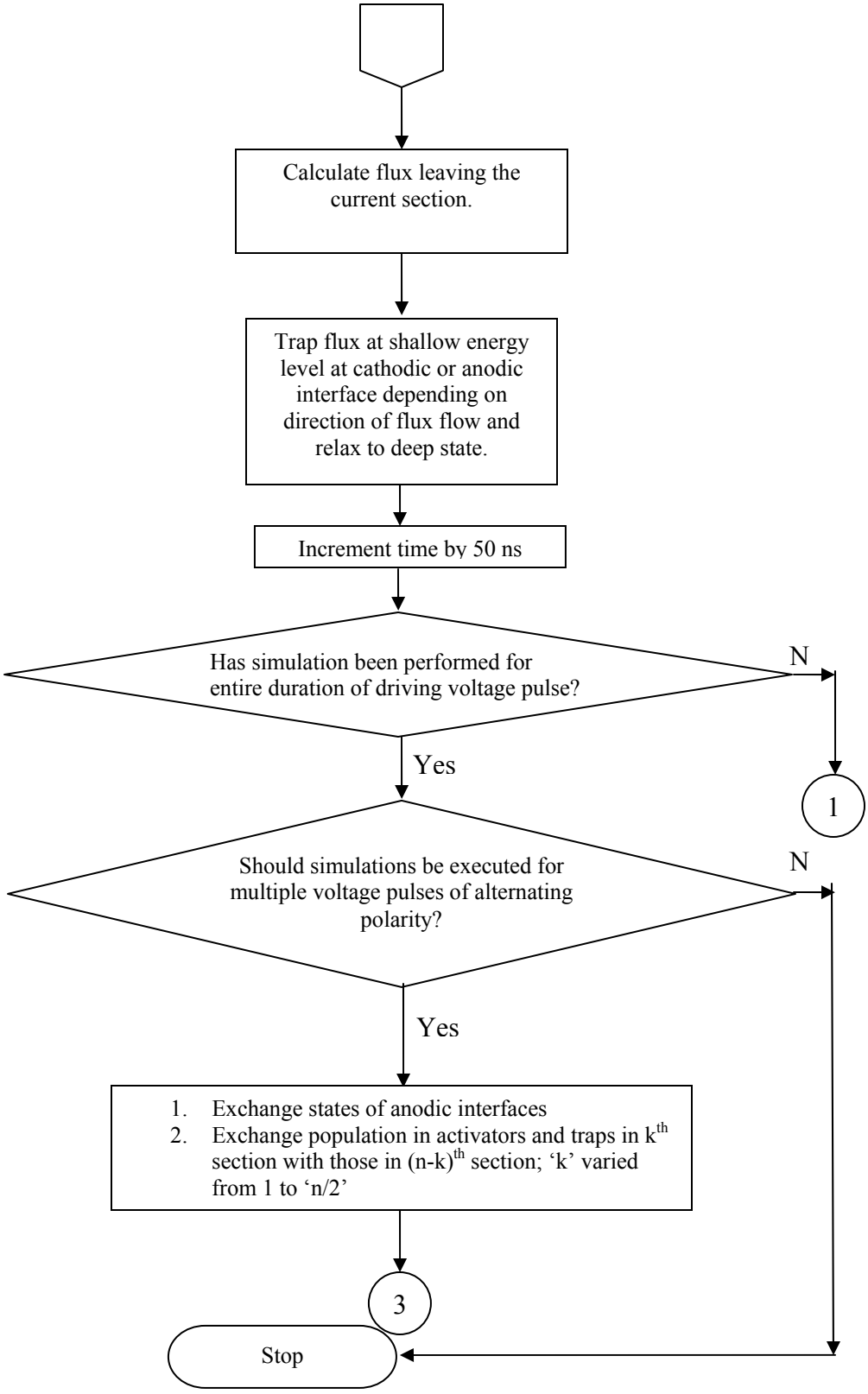

Figure 2.0.2 : Flow Chart for the Simulated Program

The flowchart used for the simulation program is shown above. The flowchart describes the systematic flow of the procedures used in the program. The values of device parameters and constants used for simulations in this thesis are as follows:

E_{sc} = shallower interface state energy level = 0.4 eV; E_{dc} = deeper interface state energy level = 0.74 eV; E_1 = bulk trap level = 0.4 eV; E_H = higher activator energy level = 0.9 eV; E_L= lower activator energy level = 3.6 eV; all energy levels are referenced from the bottom of the conduction band of SrS; n_{sc} = electron density in the shallower interface energy level = $5\text{x}10^{14}$ cm^{-2}; n_{dc} = electron density in the deeper interface energy level = 10^{16} cm^{-2}; N_{t0} = bulk trap concentration = 10^{19} cm^{-3}; N_{a0} =activator concentration = 10^{19} cm^{-3}; E_{min} = Electric field below which dipoles collapse = 1.3 MV·cm^{-1}; τ_d = activator relaxation time = $10\text{x}10^{-6}$ s; v_{th} = thermal velocity = $2.33\text{x}10^{7}$ cm·sec^{-1}; v_{sat} = saturation velocity = 10^{7} cm·sec^{-1}; S_{nt} = capture cross section area of the activator = 10^{-16} cm^{2}.

Chapter 3

Summary of Model

A schematic of the device is shown in Fig. 3.0.1. Under bipolar voltage pulse excitation, SrS based ACTFEL devices show a leading edge and trailing edge luminance peak under high voltage. Many SrS:Cu ACTFEL devices, however, exhibit not only the LE luminance peak but also two other luminance peaks, one at the beginning of the trailing edge (BTE) and the other in the middle of the trailing edge (MTE) of the voltage pulse (see Fig. 3.0.2). In addition, the LE luminance can have two peaks instead of one peak.

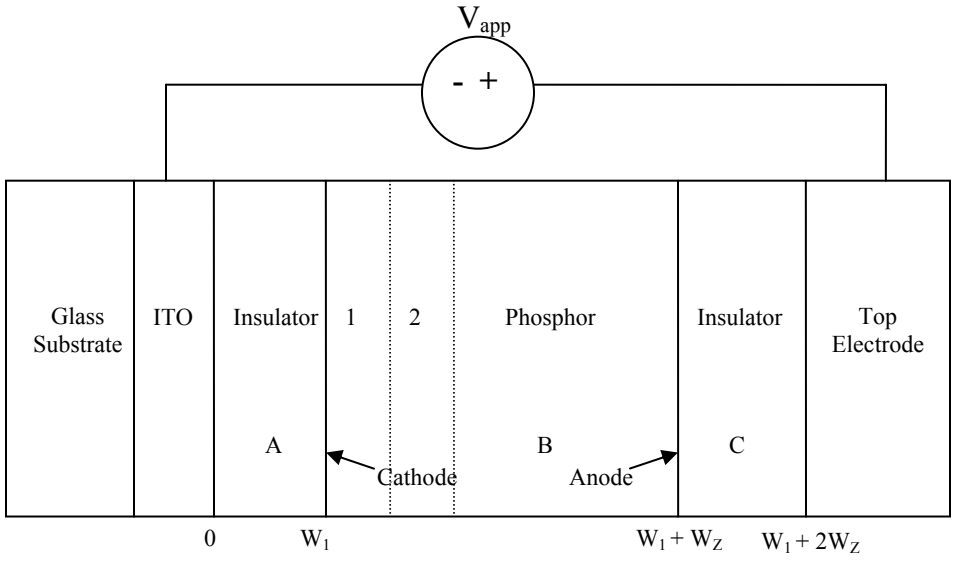

Figure3.0.1: Schematic of a SrS:Cu,Ag ACTFEL Device

We observe that at $t = t_1$, the electric field in the phosphor is large enough to tunnel-eject electrons from the insulator-phosphor interface at the cathodic end and to accelerate them to a high enough energy to cause impact excitation of Cu activators; subsequent relaxation of activators produces luminance. We call the luminance emission

during this time the leading edge (LE) luminance. As electrons travel from one end of the phosphor layer to the other, they cause not only impact excitation, but also impact ionization of Cu activators before reaching the anodic interface and getting trapped in the shallower and deeper interface states there. The ionization process creates bulk space charge that causes spatial variations in the electric field. This spatial variation in the electric field plays an important role in understanding the behavior of SrS:Cu devices. After impact ionization, the released electron can end up in (i) the conduction band of SrS or, (ii) be trapped by a "daughter "bulk trap in the vicinity of the activator, thus creating an electric dipole.

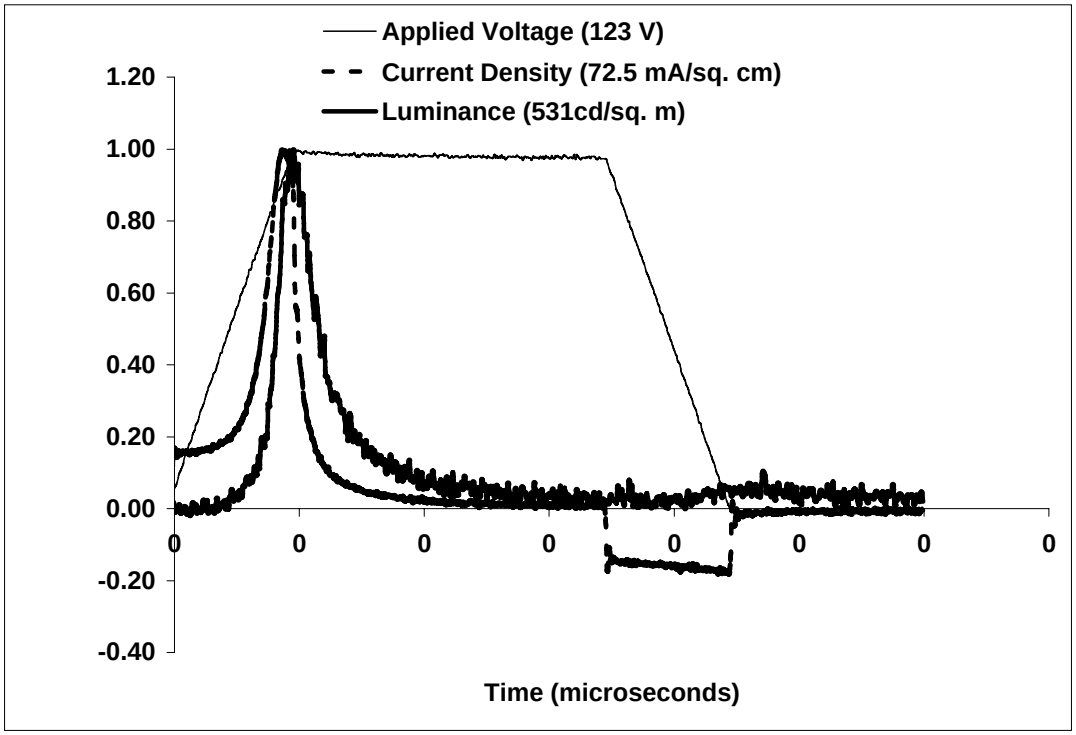

Figure3.0.2: Experimental Voltage, current and luminance waveforms for a SrS:Cu ACTFEL device for V_{amp}=123V

There is a minimum threshold field E_{min} needed to maintain the dipole; below this field, the dipole collapses. A field greater than E_{min} would be present at the leading edge

when the dipoles are created, but when the bulk phosphor field goes below this E_{min}, the ionized activator recaptures the electron from its daughter trap. This results in the annihilation of the dipole and the eventual emission of a photon when the activator relaxes. Furthermore the net phosphor field decreases substantially, just after the beginning of the trailing edge (BTE), when $t = t_2$. As a result, more bulk dipoles collapse and photon emission leads to the luminance peak termed BTE.

As the applied voltage continues to decrease, at some time t_3, the net electric field at the anodic end of the phosphor layer becomes zero. Thus, in the middle of the trailing edge (MTE), when $t_3 < t < t_4$, the net electric field there is negative and electrons are therefore released from the shallow trap levels at the anodic interface states. These electrons recombine with the ionized activators near the interface and yield the luminance peak MTE.

Chapter 4

Comparison of Simulated Field; Current and Luminance with Experimental Data for Steady State measurements

Using the procedure described in Chapter 3, electric field, current and luminance were calculated in the phosphor layer of the SrS:Cu ACTFEL device is shown in Fig. 4.0.1. Steady state waveforms for the applied voltage, luminance, current and electric field at the cathodic interface and the anodic interface are shown in Fig 4.0.3.

In Fig 4.0.1, Fig. 4.0.2 we note that **the current and luminance peak at the same time with the voltage**.

This is explained in terms of exhaustion of excitable activators as follows:

The flux ejected from the interface impacts the copper activators causing excitation and ionization processes. The excitation process is followed by relaxation within the copper activator. However, the number of activators available for impact decreases with each impact process. Thus, at some later time, a smaller number of unexcited and un-ionized activators are available for impact. Hence, any subsequent increase in flux has a reduced effect on the light emitted by the device. Consequently, luminance reaches its maximum value before current does and begins to decrease even though current continues to increase.

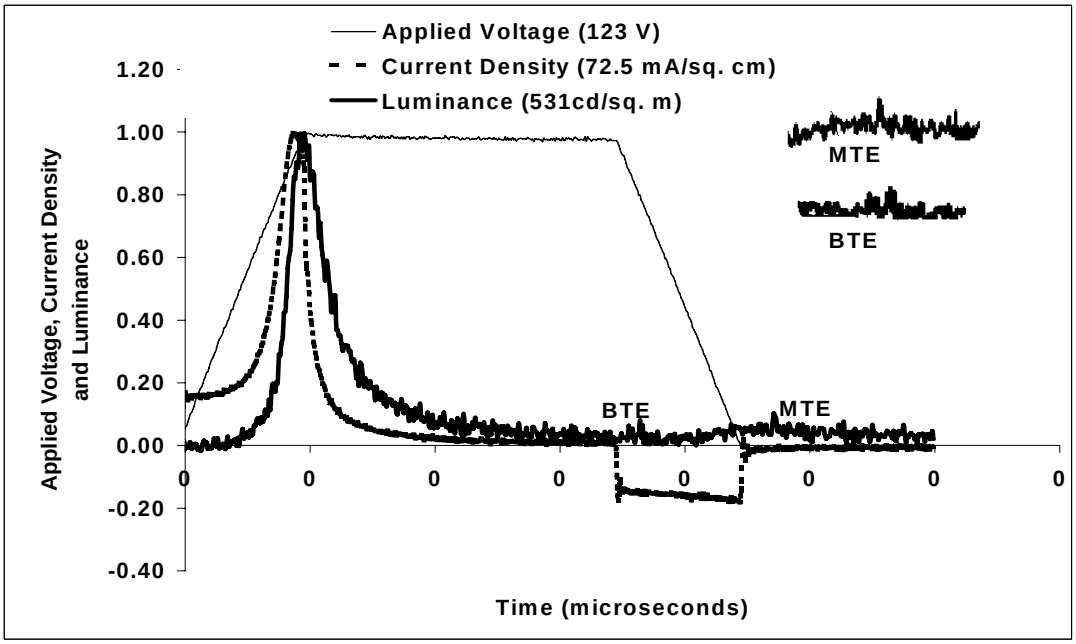

Figure 4.0.1: Experimental Voltage, current and luminance waveforms for a SrS:Cu ACTFEL device for V_{amp}=123V

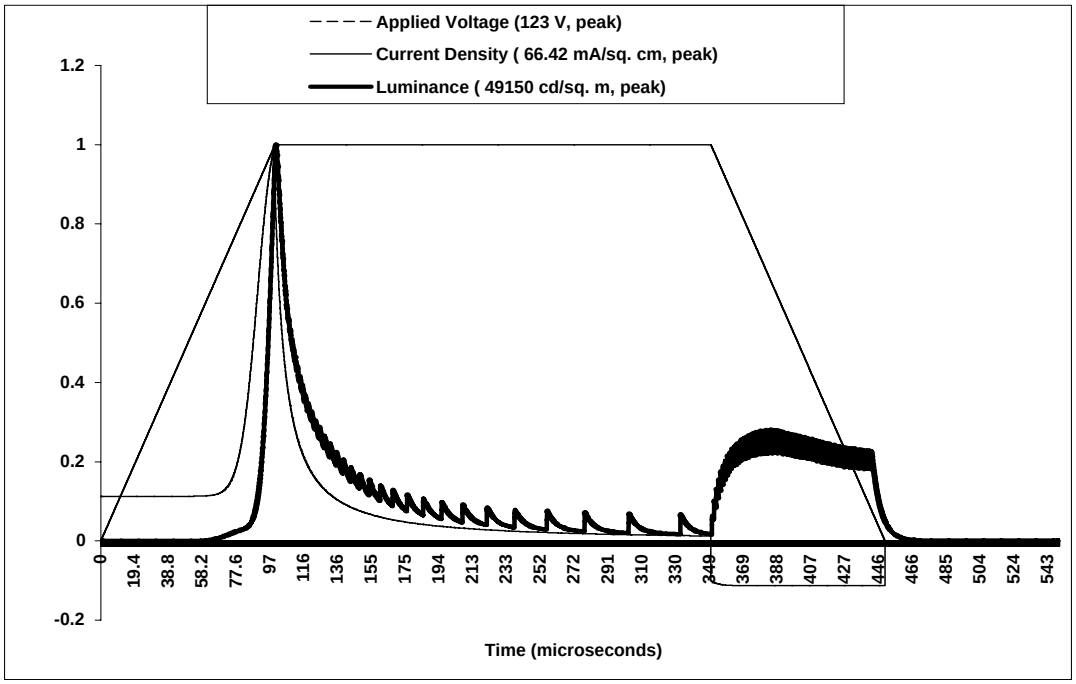

Figure 4.0.2: Simulated voltage, current and luminance waveforms for a SrS:Cu ACTFEL device for V_{amp} =123 V

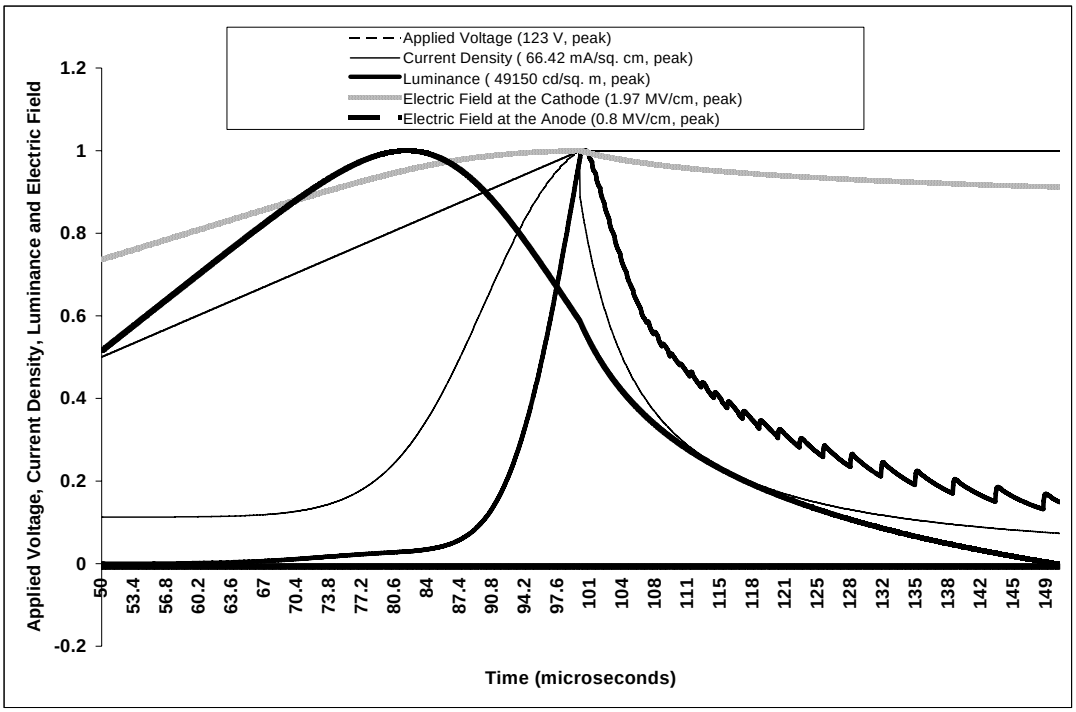

Figure 4.0.3: Detail of simulated voltage, current, luminance and electric field of Fig. 4.0.2.

In Fig. 4.0.1, the BTE luminance did not exhibit a single smooth rise and fall curve like leading edge luminance did; instead it was made up of several closely spaced peaks. The jagged BTE waveform is attributed to spatial variation of electric field within the phosphor. The BTE luminance is produced due to the collapse of dipoles, and subsequent relaxation of the electron within the activator. The time of collapse is determined by the time at which the net electric field in the phosphor goes below a threshold field. For the purpose of simulations, the phosphor was divided into 100 sections. The electric field varied spatially across the sections. Hence, the dipoles collapse at different instances of time in different sections in phosphor. As a result, we get many closely spaced peaks.

The third luminance peak (MTE) occurs in the middle of the trailing edge. At this time also reverse tunnel current appears. This reverse tunnel current arises when the net field at the anodic interface is high enough to cause tunneling of electrons at the anode back into de conduction band. As these electrons go into the conduction band they can cause luminance through two processes: i) impact excitation of activators followed by relaxation. This process does not have a low probability of occurrence since the "reverse" field is high enough to cause tunneling, it should also be high enough to cause impact excitation ii) recapture of electrons by ionized activators. Although in either case, a reverse tunnel current should be observed, it is small compared to the "forward" tunnel and displacement currents.

Quantitative Match:

1. The light collected by the optical cable couples to the spectrometer, PMT and finally to the DSO.

2. The luminance (as seen by the eye) is measured using a photometer for different voltages.

3. Since the total luminance per second = photometer value, we can calculate the peak value of luminance, i.e., =photometer value.

f = 100 Hz, dt = 1 μs.

4. Calculate h and find the peak value = h.

Structure of the Data File

Column 1: Time

Column 2: Applied Voltage (V)

Column 4: Luminance (PMT output (Amps))

Column 5: Current (100x Amps)

The column 4 and 5 usually needs to be corrected for bias.

The column 4 is luminance and the values are negative because a negative bias is applied to the PMT.

Calculating Applied Voltage

Experimental

The second column of the data file gives the voltage applied to the device in Volts.

Theoretical

The First column of the data file gives the voltage applied to the device in Volts.

Calculating Peak Luminance (L)

Experimental

The luminance is calculated as follows:

The photometer measures the value of luminance as seen by the eye (by compensating using the photo-optic curve) per second.

The fourth column in the data file is the luminance as measured by the spectrometer at each 'dt', then converted to current by the PMT.

We will obtain a correlation between the data in column 4 and the value of luminance measured using the photometer.

Total luminance as read by the spectrometer per second is obtained by

- Adding the total luminance for 2 pulses (10000 microseconds) …(1)

- Multiplying this sum by f (100 Hz) and dt (1 microsecond)…(2)

We equate the result of 2 to the luminance value read by the photometer. …(3)

We find the peak value of the column 4, which is the peak value of luminance as measured by the spectrometer, and converted to current by the PMT …(4)

If (3) holds, then what is the peak value in cd/m2?

Peak value in cd/m2 = [Peak value (from column 4) * Luminance read by the photometer]/Result of (2)

Theoretical

The peak luminance was calculated by finding the maximum of the luminance values obtained by simulating the rate equations and the luminance equation (L(t) = B. nah. Wx/Tau).

Calculating Peak Current

Experimental

In order to detect the low current flowing through the device, the current is multiplied by passing it through a 100 loop coil and reading the resultant current on the oscilloscope; the collected current is divided by the area of the dot on the device in order to determine the current density, and divided by 100 to arrive at the correct result (A/sq. cm)

Theoretical

The flux, as determined by the rate equations, is multiplied by charge (q (C)) to obtain the current density (C/sq. cm .s = A/sq. cm).

Calculating Total Luminance

Experimental

Using a photometer, the experimental luminance averaged per second was collected (cd/sq. m).

Theoretical

The theoretical total luminance was obtained by integrating the luminance emitted per unit second over the time duration of luminance emission (cd/sq. m). (sum all the luminance and multiply by 50 ns)

Calculating Total Charge

Experimental

The total charge transferred was calculated by multiplying the total time during which conduction current flows in the device with the sum of currents flowing at every dt (1 microsecond).

Theoretical

The total charge transferred was calculated by multiplying the total time during which conduction current flows in the device with the sum of currents flowing at every dt (50 nanoseconds).

The benchmark we have assumed to be 123V (Fig. 4.0.1 and Fig. 4.0.2). We now determine the current and luminance values for both the experiments and the simulations.

Current value for the experimental data is given by:

The maximum current produced was found out to be 0.6012A, we use 100 coils

- 5437/100 = 6.012mA

- The total current produced will be 5.4375/0.075 = 75 mA/cm^2
- (Area of the dot = $\pi d^2/4$, diameter of the dot is given by 2.54 cm, thus the area was found out to be 0.075)

Thus the **total current** was experimentally found out to be **72.5 mA/cm^2**

The measured and the *simulated peak currents* are **72.5 mA/cm^2** (experimental) and **66.42 mA/cm^2** (theoretical) for $\mathbf{V_A}$ **= 123 V**. *Experimental and theoretical charge* transferred per pulse were **2.75 μC/cm^2 and 2.26 μC/cm^2.** *Peak experimental and simulated luminance* values for $\mathbf{V_A}$ **= 123 V** case were **531 cd/m^2 and 49150** cd/m^2 respectively. *Total experimental and simulated luminance* values for $\mathbf{V_A}$ **= 123 V** case were **6.2 cd/m^2 and 561.2 cd/m^2** respectively. Due to internal reflections in the device, losses occurred during luminance collection during measurements. The variation between experimentally observed and simulated luminance can be attributed to the following factors: (i) we have not accounted for the distance an electron must travel (after each impact) to regain enough energy for impact excitation/ionization. (ii) clustering effect of activators and its impact on luminance (iii) quenching because of neighbor defect and (iv) quenching because of concentration. Hence, we have defined a parameter called optical loss factor, k, whose value can be varied according to the specifics of the particular experiment. The optical loss factor takes into account the factors for lower luminance listed above.

The voltage amplitudes were varied over a wide range of values and the theoretical values of peak luminance, peak current, total luminance and total charge transferred were compared with the experimental values; the results were nearly proportional for different

device excitation parameters. The effects of voltage amplitude, activator concentration, interface energy levels, and critical field for dipole collapse were studied. These simulations showed that secondary (after the main peak) luminance peaks can be produced by: i) electron "backflow" from the cathodic interface when the magnitude of the applied voltage pulse decreases and by ii) ionized activators recapturing "their" electron from a neighboring trap.

Effects of Varying Drive Voltage Amplitude

Procedure:

Voltage pulses of varying amplitude were applied to the device and different sets of data were collected. Simulations were performed by applying different voltages to the device and the data on the resulting flux and luminance was collected for each of these voltages.

In our study, the applied voltage values were 123V, 127V and 132V. Experimental, current and luminance waveforms for V_{amp} values of 127V and 132V are shown in Fig. 4.0.4, and Fig. 4.0.6. Simulated, current and luminance waveforms for V_{amp} values of 127V and 132V are shown in Fig. 4.0.5, and Fig. 4.0.7. At low voltages (V_{amp} < 123V), no appreciable conduction current is seen. Due to low applied voltage, the net electric field in the phosphor is far too low to make the ejected electrons numerous or energetic enough to impact excite the activators; yet it is high enough to field-ionize the activators and thus create dipoles. BTE luminance is emitted when the activator-trap dipoles relax.

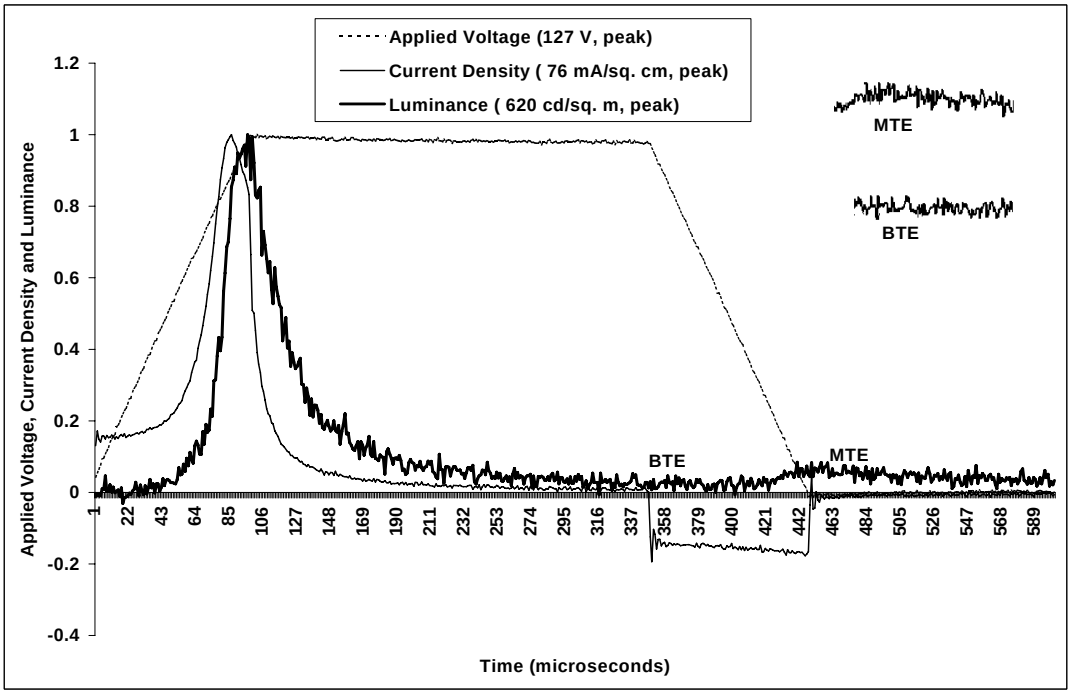

Figure 4.0.4: Experimental Voltage, current and luminance waveforms for a SrS:Cu,Ag ACTFEL device for V_{amp}=127 V

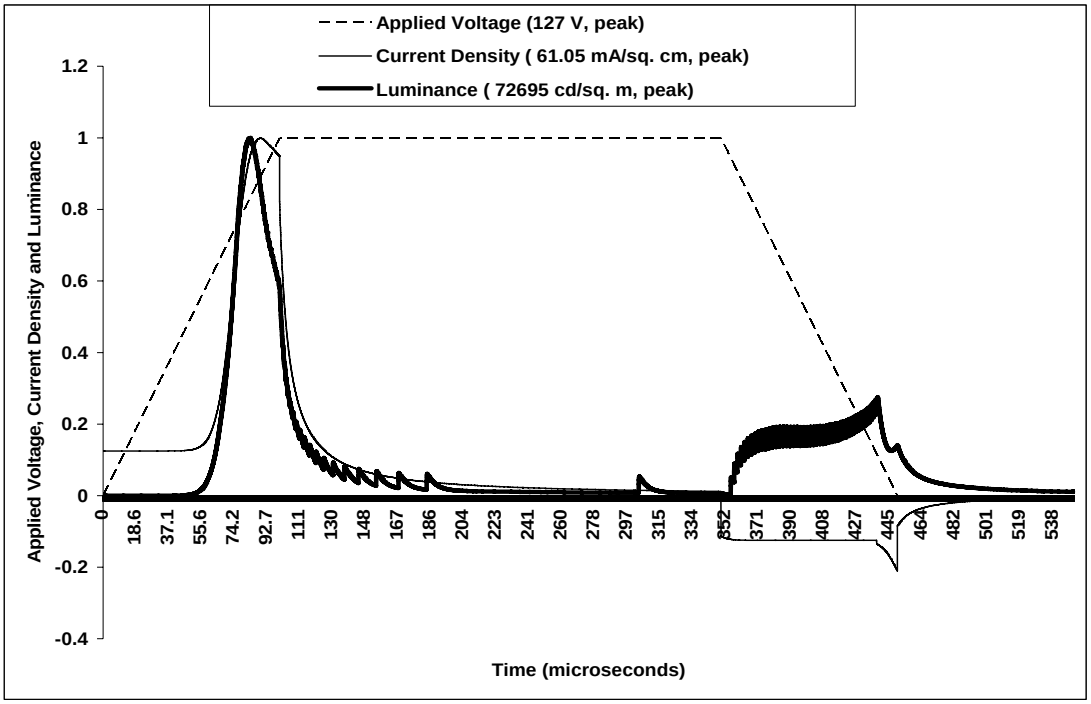

Figure 4.0.5: Simulated Voltage, current and luminance waveforms for a SrS:Cu ACTFEL device for V_{amp}=127 V

As the voltage amplitude is increased both current and luminance increase. It is interesting to note than even though a higher voltage is applied, the spatial average of the field in the phosphor layer is not higher, as one might intuitively expect.

In Fig 4.0.4, Fig. 4.0.5 we note that **the current reached its maximum value much earlier than voltage**. It is attributed to the following processes occurring in the device:

The electric field applied to the device increases as the voltage applied to the device increases. When the threshold electric field for tunneling from interface states is reached, electrons tunnel out of the insulator-phosphor interface and reach the other interface. On their path, the electrons collide with the activators and ionize them. As a result, there is a positively charged interface (from which the electrons have tunneled out), positively ionized activators in the bulk of the phosphor (ionized upon impact by the hot electrons) and a negatively charged interface (as a result of trapping the electron flux). Hence, an internal electric field builds up in the phosphor and the direction of this internal field is opposite to the direction of the applied electric field. The rate of increase of internal electric field is dependent upon the rate at which flux is ejected from the interface, the rate at which impact ionization occurs in the phosphor and the rate at which electron is transferred from one interface to another.

From this we see that the electric field at the cathodic interface and the current reach their maximum at the same time (t_6). Cathodic field then clamps and remains

constant until t = t_7 when the applied voltage stops rising. After t7 cathodic field decreases. Thus between t6 and t7 the rate of increase of cathodic field due to the rising voltage is exactly counteracted by the rate of increase in the internal field at the cathode. However the electric field at the anodic interface (and in the bulk phosphor layer) is smaller and in continuing to decrease. As a result the electron flux from impact ionization of activators is also decreasing and hence the total phosphor current starts to decrease after t6 even though the cathodic field does not decrease until t7. Thus, under the assumption of an infinitely large interface state electron population, experimental observations of current peaking before the voltage can serve as evidence for ionization of activators or traps in the bulk phosphor layer. If the interface state electron population is not infinitely large, and is subject to exhaustion, then, of course, the reduction in current between t6 and t7, in spite of constant cathodic field, could be attributed to reduced tunnel current resulting from reduced interface electron population.

On observing the ***luminance characteristics*** in Fig. 4.0.5 **we find that the luminance reached its maximum value earlier than current did**. This is explained in terms of exhaustion of excitable activators as follows:

In Fig. 4.0.5, we see that the flux ejected from the interface impacts the copper activators causing excitation and ionization processes. The excitation process is followed by relaxation within the copper activator. However, the number of activators available for impact decreases with each impact process. Thus, at some later time, a smaller number of unexcited and un-ionized activators are available for impact. Hence, any subsequent

increase in flux has a reduced effect on the luminance emitted by the device. **Consequently, luminance reaches its maximum value before current does and begins to decrease even though current continues to increase.**

The BTE luminance is produced due to the collapse of dipoles, and subsequent relaxation of the electron within the activator. The time of collapse is determined by the time at which the net electric field in the phosphor goes below a threshold field. The third luminance peak (MTE) occurs in the middle of the trailing edge. At this time also reverse tunnel current appears. This reverse tunnel current arises when the net field at the anodic interface is high enough to cause tunneling of electrons at the anode back into de conduction band. As these electrons go into the conduction band they can cause luminance through two processes: i) impact excitation of activators followed by relaxation. This process does not have a low probability of occurrence since the "reverse" field is high enough to cause tunneling, it should also be high enough to cause impact excitation ii) recapture of electrons by ionized activators. Although in either case, a reverse tunnel current should be observed, it is small compared to the "forward" tunnel and displacement currents.

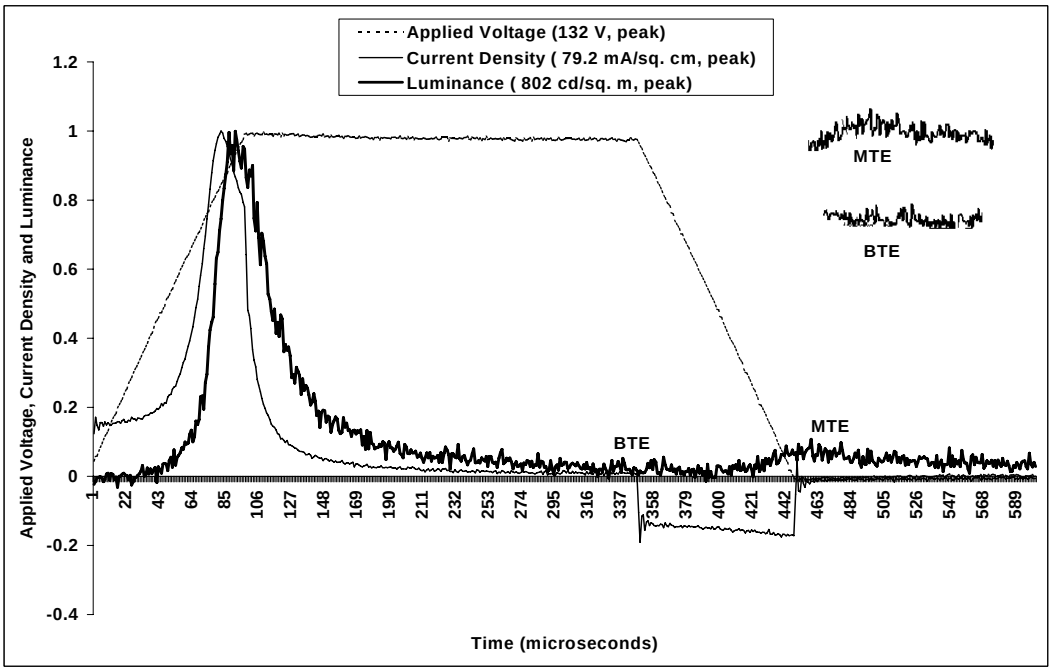

Figure 4.0.6: Experimental Voltage, current and luminance waveforms for a SrS:Cu ACTFEL device for V_{amp}=132 V

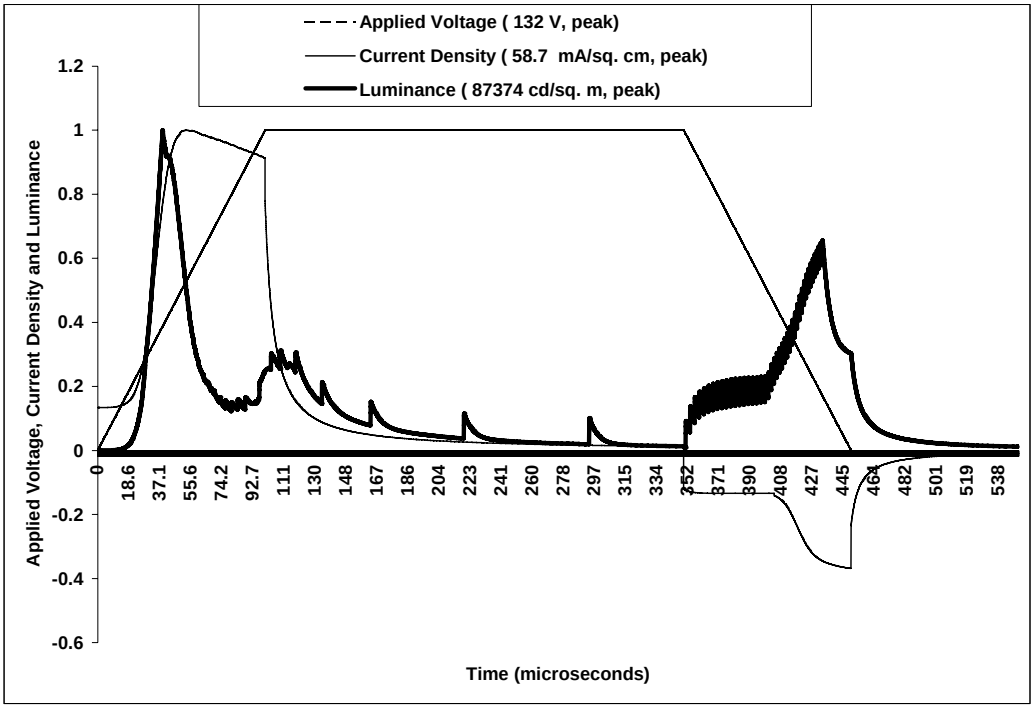

Figure 4.0.7: Simulated Voltage, current and luminance waveforms for a SrS:Cu ACTFEL device for V_{amp}=132 V

The electric field in the device due to the applied voltage is high and hence, electrons tunnel from the interfaces much earlier. As a result of rapid transfer of charges from one interface to another, the internal electric field builds up quickly and hence, flux peaks much earlier when compared to earlier plots (Fig. 4.0.7 and Fig. 4.0.8).

Luminance, produced as a result of impact excitation process, tracks the flux waveform until time "t_1", after which it exhibits a shoulder. This shoulder is attributed to the phenomenon of collapse of dipoles, caused by the decreasing electric field at the anode and sections nearer the anode. Subsequent dipole collapse in the sections nearer the cathode and ultimately, at the cathode manifests itself as the jagged BTE luminance peaks.

Since the applied voltage is higher and has a greater rate of increase (compared to 4.0.2), a greater and rapidly rising electric field is applied to the device. This electric field causes the flux of electrons to tunnel out of the cathodic interface more rapidly and this, in turn, causes the internal electric field to increase very rapidly. Such a rapid rate of increase in the internal electric field causes the net field to decrease much earlier and hence, the flux exhibits a peak.

The luminance curve tracks the flux curve; it is, however, noted that the luminance curve exhibits a rounded LE peak unlike the previous Fig. 4.0.6. On closer observation, it is noted that this rounded peak is made up of many small jagged peaks. This is explained as under:

Since the net electric field decreases much earlier (the flux peaks much earlier too), the critical electric field required to maintain the dipole is no longer present in the device. Hence, the dipoles begin to collapse much earlier and hence, at time instant "t_1", the total luminance is made up of 2 components:

1. Luminance produced due to the impact excitation of activators.
2. Luminance produced due to the collapse of dipoles.

As a result of these two components, the peak is neither sharp nor smooth; the peak is rounded and jagged.

As explained previously (Fig. 4.0.1), increase in applied voltage increases the electric field applied to the device and consequently the flux flows much earlier and peaks much earlier due to the rapidly increasing internal electric field.

When the applied voltage is held constant at 132V, the applied electric field is constant throughout the device; the net electric field is decreasing rapidly and this is noticed from the change in slope of the flux waveform.

ACTFEL devices are almost always operated by applying bipolar pulses. The amplitude of these pulses, which we call V_{amp}, is an easily varied operation parameter that can control the magnitude as well as the characteristics (presence or absence of peaks) of the luminance waveform. Our reference condition is V_{amp} = 123 V.

Threshold Voltage versus Luminance

Luminance is the ratio of the luminous intensity in a given direction of infinitesimal elements of a surface containing the point under on a plane perpendicular to the given direction. The luminance is measured by a photometer. The luminance is a photometric term indicating the radiated power in terms of human eye sensitivity. The physical measure of the luminous intensity is cd/m^2. It is often being referred to as fL (foot lamberts).

$$1fL = 1/pi * cd / (ft)^2 = 3.426\ cd/m^2$$

Threshold voltage is defined as the voltage corresponding to the luminance of 1 cd/cm^2. Figs. 4a and 4b show the experimental and simulated L-V curves at different voltages. It is seen that the ratio of total luminance emitted per pulse at various voltages between experimental and simulated values is almost constant. The experimental luminance is lesser than simulated luminance because factors such as internal reflections in the device, losses occurring during luminance collection are not yet incorporated into the model; moreover, we have not accounted for (i) the distance an electron must travel (after each impact) to regain enough energy for impact excitation/ionization. (ii) the clustering effect of activators and its impact on luminance (iii) the quenching because of neighbor defect and (iv) the quenching because of concentration. Hence, we have defined a parameter called optical loss factor, k, whose value can be varied according to the specifics of the particular experiment. The optical loss factor takes into account the factors for lower luminance listed above.

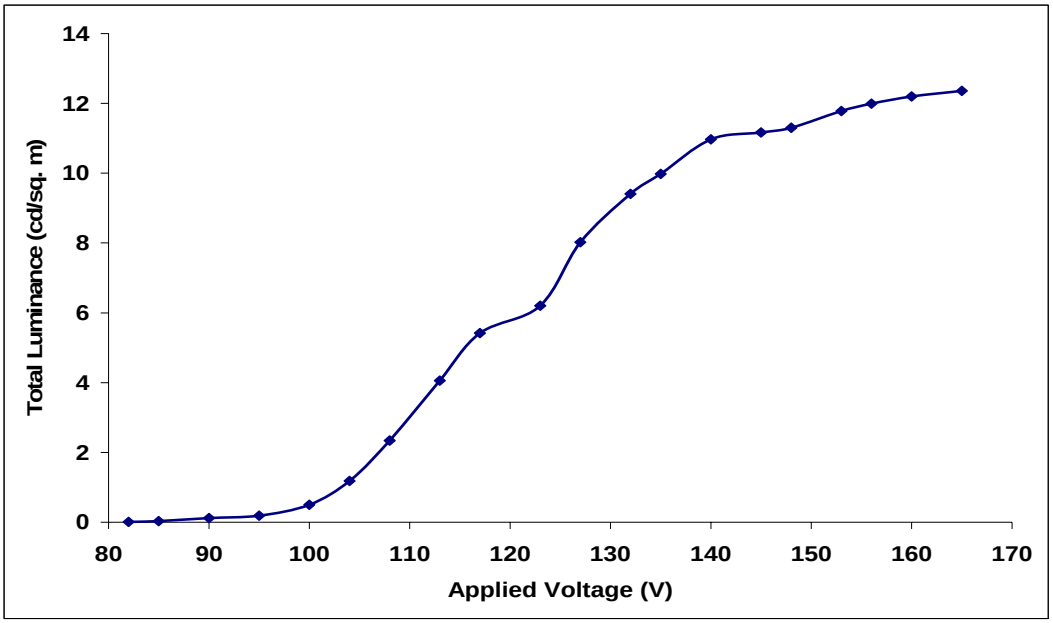

Figure 4.0.8: Experimental Total Luminance-Voltage (cd/sq.m) characteristics of the SrS:Cu ACTFEL device with rise time = fall time = 100 μs.

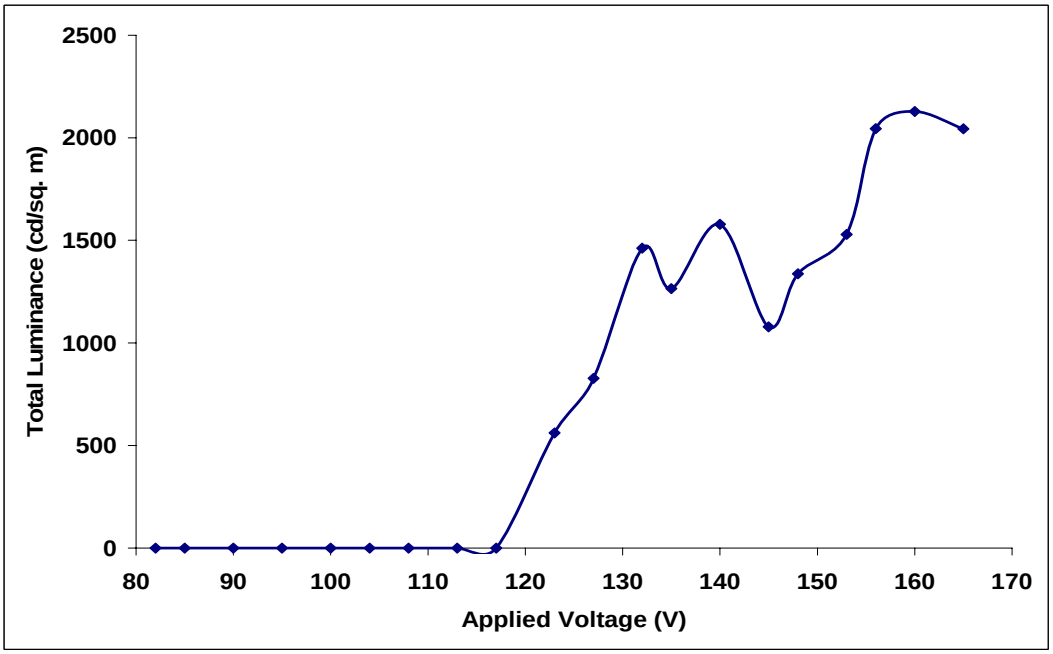

Figure 4.0.9: Simulated Total Luminance-Voltage (cd/sq.m) characteristics of the SrS:Cu ACTFEL device with rise time = fall time = 100 μs.

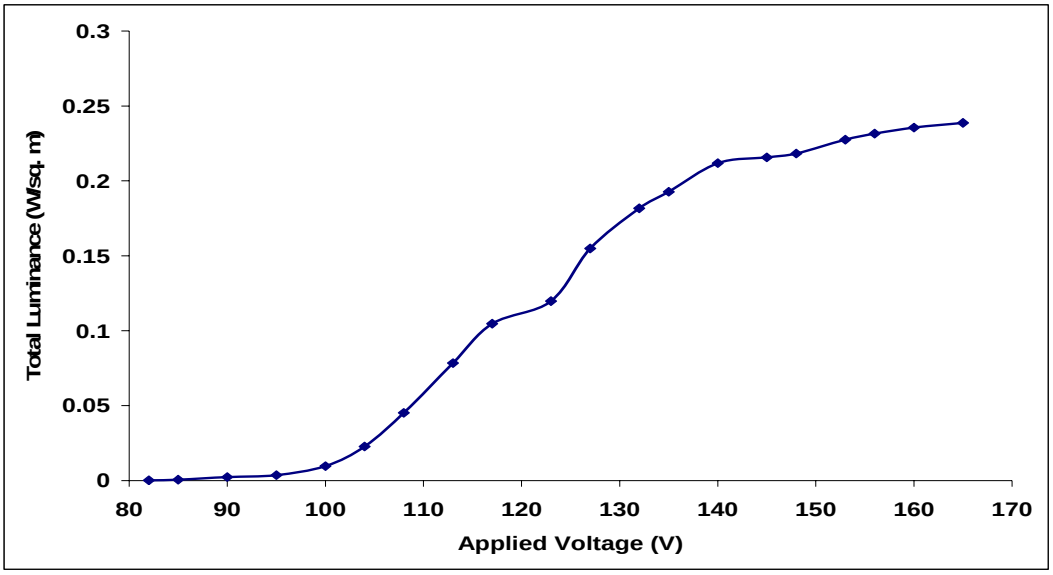

Figure 4.0.10: Experimental Total Luminance-Voltage (W/sq.m) characteristics of the SrS:Cu ACTFEL device with rise time = fall time = 100 μs.

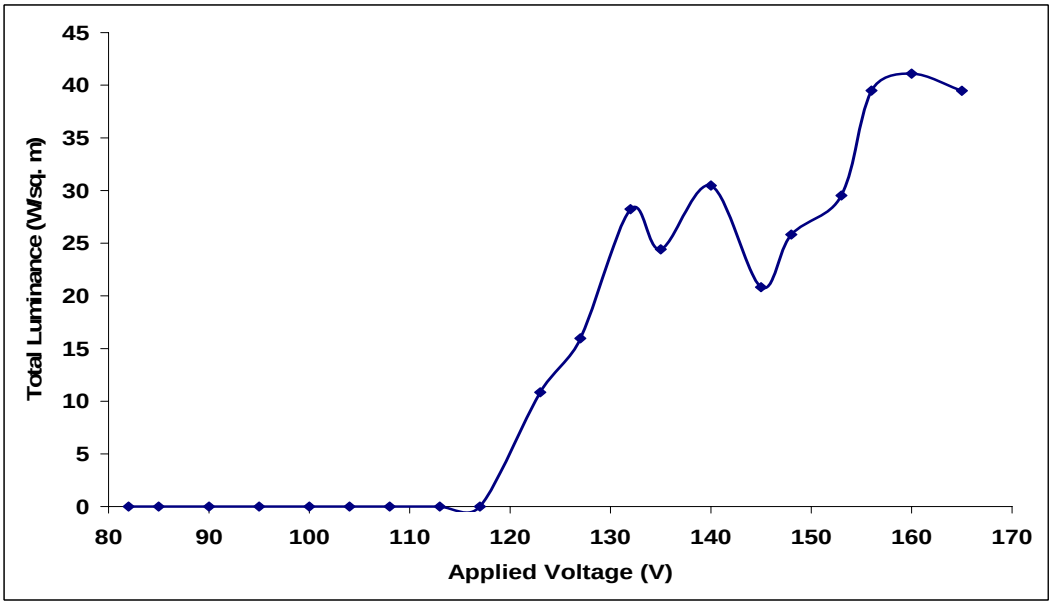

Figure 4.0.11: Simulated Total Luminance-Voltage (W/sq.m) characteristics of the SrS:Cu ACTFEL device with rise time = fall time = 100 μs.

Simulated versus Experimental L-V

The EL emission mechanism is generally accepted for ZnS – based EL devices. In SrS- based EL devices; however an additional mechanism has been included. The field-induced ionization of luminescent centers and subsequent trapping of low energy electrons, resulting in the EL emission characterize the additional mechanism.

The typical curve shows simulated and experimental luminance versus Voltage characteristic curves of the SrS:Cu device. This L-V curve features a threshold voltage Vth below which a little luminance is emitted, a steeply rising characteristic above threshold, and finally a saturation region. The threshold voltage is defined by the voltage corresponding to the luminance of 1 cd/m^2. As indicated in the figure, the Vth is 90 V in case of the experimental value and the typical value for a simulated voltage is around 115 V. This highly non-linear L-V characteristic provides a device with a capability to be electrically addressed at a very high multiplexing ratio while maintaining excellent contrast. This phenomenon is what makes is required for the matrix addressing of high-information content in flat panel displays.

Above the threshold voltage, Luminance rises rapidly because of increased transfer charge in the phosphor layer. The sharp increase in luminance is due to the tunnel injection of electrons from trap states at the phosphor layer/insulating layer interface.

It is noted that above a threshold voltage, luminance is produced; this is the voltage required to set up the electric field in the device that causes conduction current to flow. The number of activators in the device plays a crucial role in determining the amount of luminance emitted from the device; this is discussed in detail in Chapter 5.

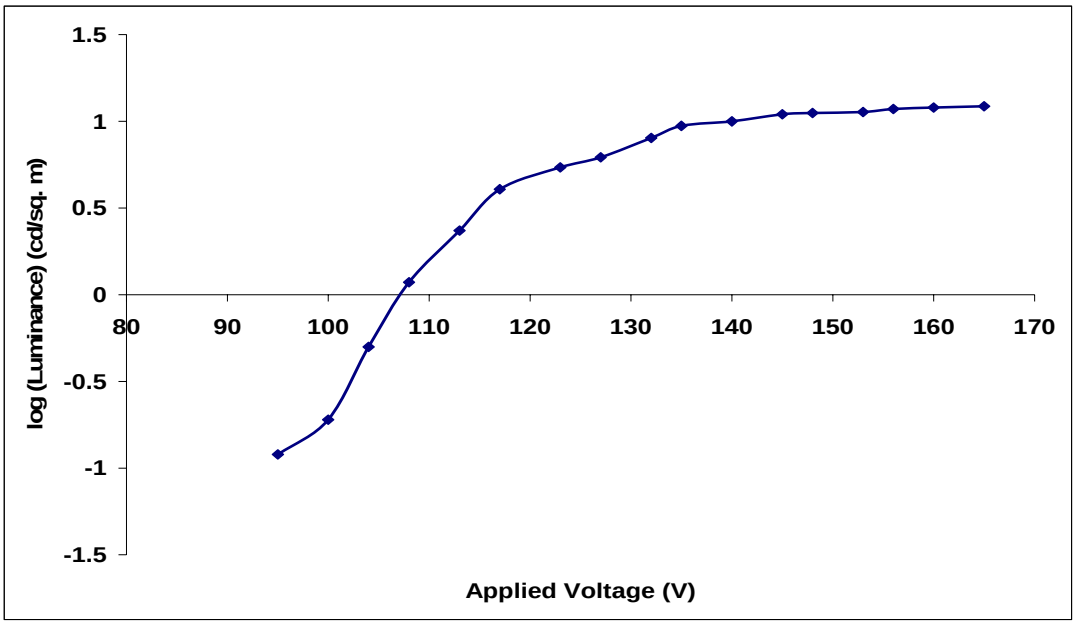

Figure 4.0.12: Experimental log(Total Luminance)-Voltage (cd/sq.m) characteristics of the SrS:Cu ACTFEL with rise time = fall time = 100 μs

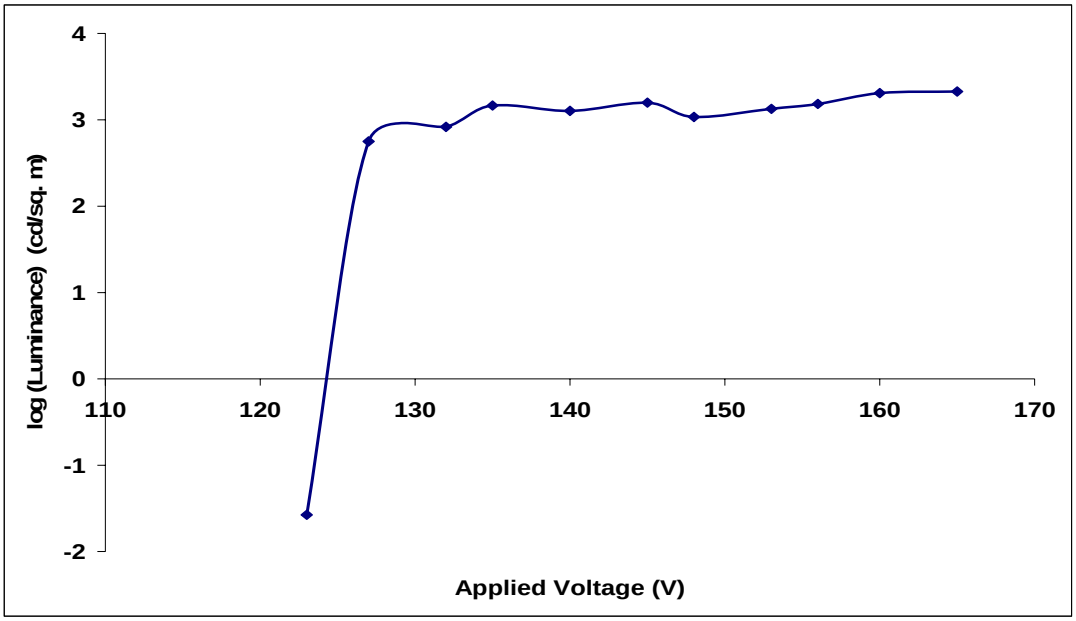

Figure 4.0.13: Simulated Total log(Luminance) -Voltage (cd/sq.m) characteristics of the SrS:Cu ACTFEL device with rise time = fall time = 100 μs.

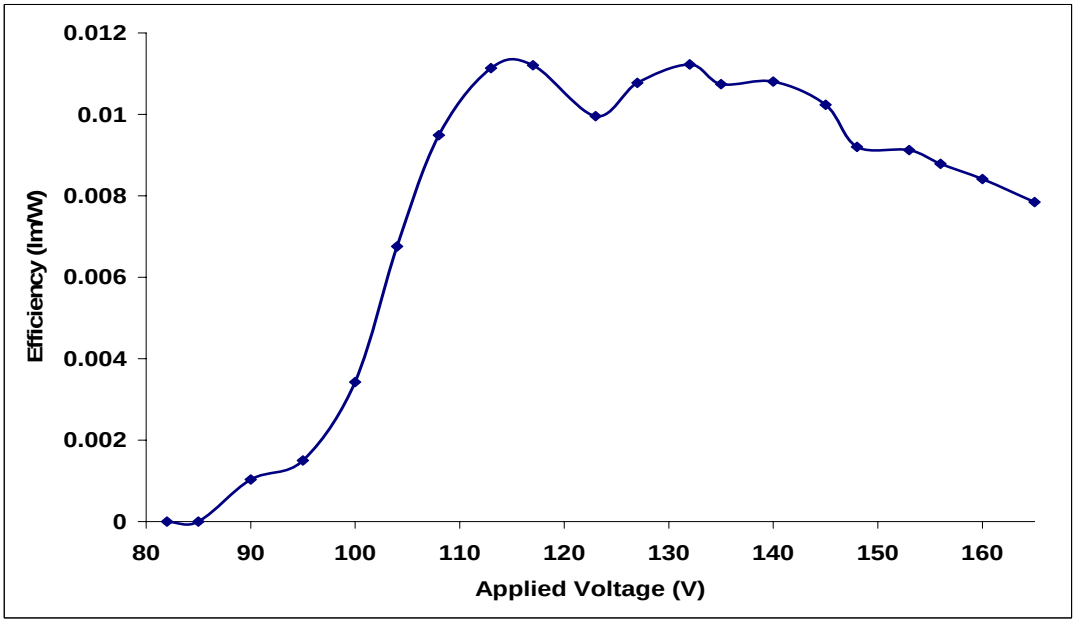

Figure 4.0.14: Experimental Efficiency-Voltage (lm/W) characteristics of the SrS:Cu ACTFEL with rise time = fall time = 100 μs.

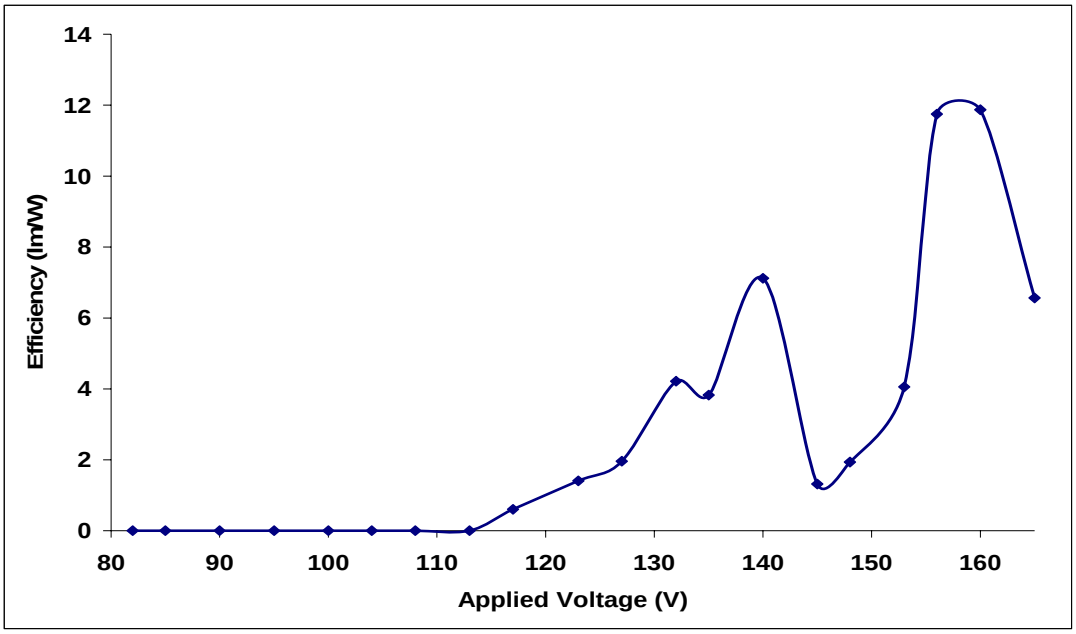

Figure 4.0.15: Simulated Efficiency -Voltage (lm/W) characteristics of the SrS:Cu ACTFEL device with rise time = fall time = 100 μs.

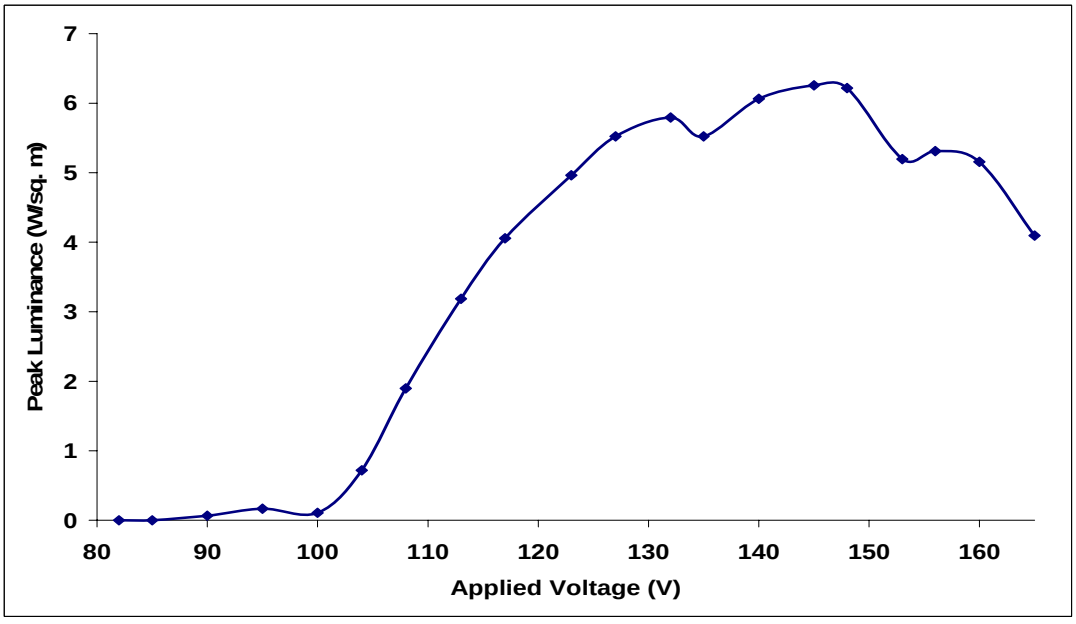

Figure 4.0.16: Experimental Peak Luminance-Voltage (W/sq.m) characteristics of the SrS:Cu ACTFEL device with rise time = fall time = 100 μs.

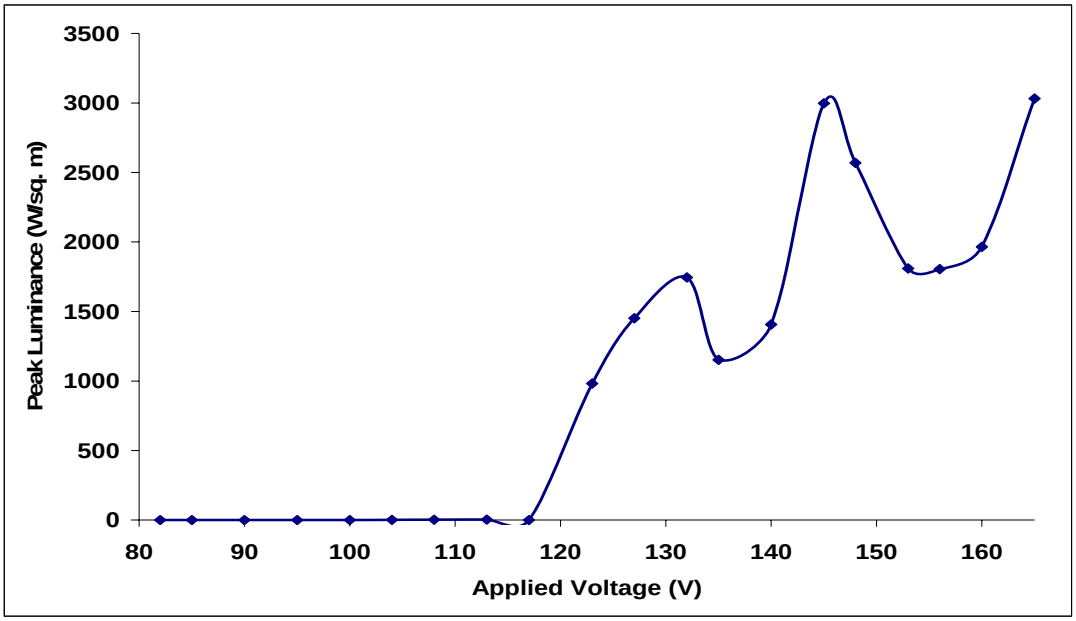

Figure 4.0.17: Simulated Peak Luminance-Voltage (W/sq.m) characteristics of the SrS:Cu ACTFEL device with rise time = fall time = 100 μs.

Charge versus Voltage-(Q-V)

The transferred charge density increases linearly as a function of voltage above the threshold voltage, which is seen more explicitly shown in linear L-V and Q-V curves for SrS:Cu device driven at 123V for the experimental and 123V in simulations.

The relationship between the Luminance and transferred charge density is depicted for the two drive frequencies, showing that the luminance L is proportional to the frequency f and the transferred charge density Q over a wide range. The proportionality constant depends on the phosphor layer properties, such as crystallinty, concentration of luminescent centers, distribution of luminescent centers and space charge.

The luminance is proportional to the transferred charge density within the phosphor layer, so that an increase in the transferred charge is bound to improve the luminance. The excitation probability of the luminescent centers by the hot electrons should be improved, where it is the function of the energy received by the hot electrons from the electric field.

The luminance produced by the device increases as voltage increases and saturates at a critical voltage; beyond this voltage, any increase in voltage does not result in a substantial increase in luminance. This is because the excitable activators have all been exhausted at this critical voltage and any further increase in voltage increases the flux of "hot" electrons but not the number of luminance producing transitions (Fig. 4.0.12, Fig 4.0.13).

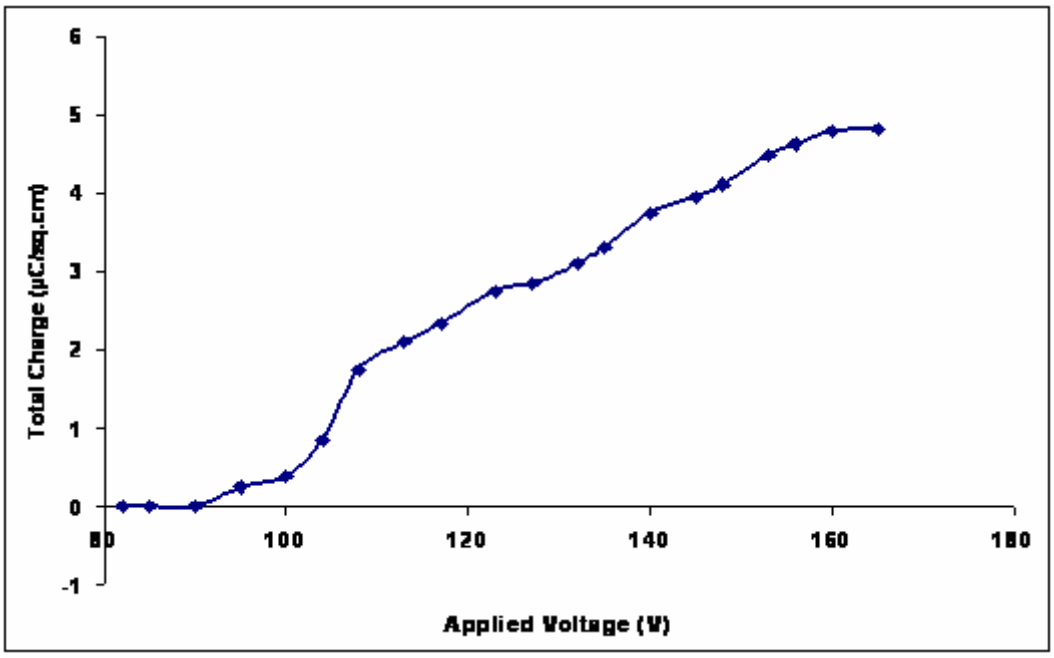

Figure 4.0.18: Experimental Total Charge-Voltage (µC/sq.cm) characteristics of the SrS:Cu ACTFEL with rise time = fall time = 100 µs.

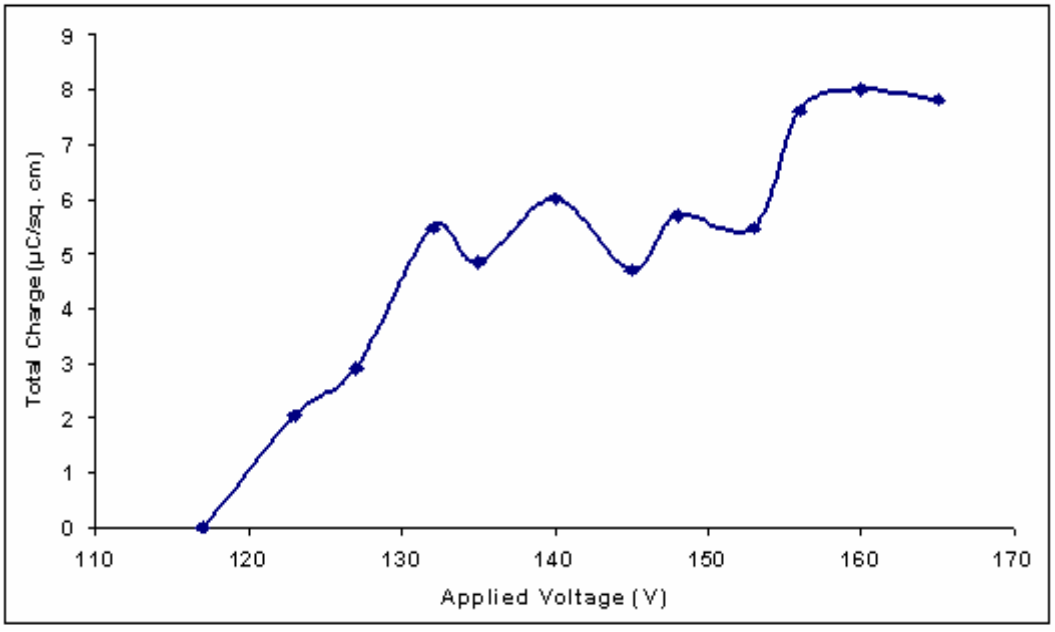

Figure 4.0.19: Total Charge -Voltage (µC/sq.cm) characteristics of the SrS:Cu ACTFEL device with rise time = fall time = 100 µs

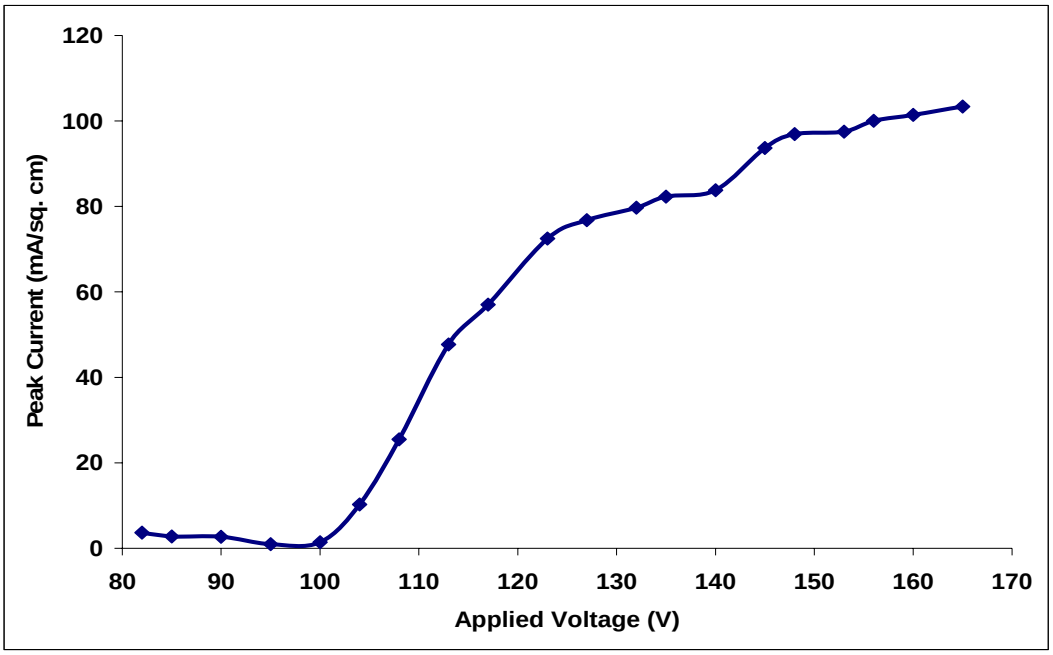

Figure 4.0.20: Experimental Peak Current (mA/sq.cm) characteristics of the SrS:Cu ACTFEL device with rise time = fall time = 100 μs.

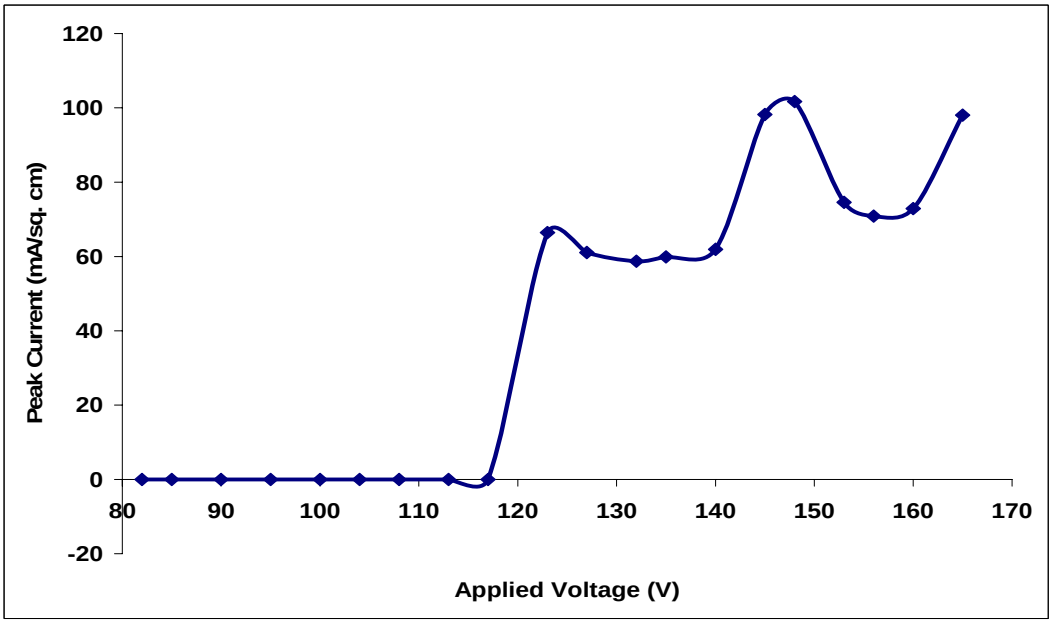

Figure 4.0.21: Peak Current -Voltage (mA/sq.m) characteristics of the SrS:Cu ACTFEL device with rise time = fall time = 100 μs.

Chapter 5

Effects of Varying Device and Drive Parameters with the Simulated Data for Steady State Measurements

Varying the values of five device and drive parameters over a wide range performed numerical simulations. These were activator concentration, depth of interface states, driving voltage amplitude, threshold electric field for dipole collapse and probability of dipole formation. The values of each of these parameters were varied one at a time so that the effect of each of these parameters on the VIL characteristics could be observed and interpreted. For all calculations in Section IV the starting point was the constants listed in Table 1 except that N_{a0} was equal 10^{19} cm^{-3}.

For this reason, as the applied field stops increasing and the built-in counter-field keeps increasing due to field-assisted-ionization of activators, the field in the phosphor near the anode, which is lower in magnitude, would go below the E_{min} necessary to maintain dipoles and dipoles would collapse and emit luminance in the form of a "shoulder" in the LE peak. This "shoulder" is clear for V_{amp} = 132 V. If most of the possible dipoles get formed even for the reference V_{amp} = 160 V case, a higher V_{amp} would not significantly increase the number of formed dipoles. This means that after the voltage ramp-up, about the same number of dipoles exist in the phosphor layer for the reference case and for higher V_{amp} conditions. Having the same number of dipoles in these cases, but with dipole collapse starting earlier in the pulse for the higher V_{amp} cases, dipole collapse will also end earlier, resulting in shorter duration of BTE at V_{amp} = 132 V.

MTE is not significantly affected when V_{amp} goes above the reference case, although it is absent for V_{amp} = 117V. However, for the sufficiently high Vamp = 132 V, "reverse" tunnel current appears, which results from electrons at the anodic interface back-flowing into the conduction band after the applied field is removed and the net field at the anode becomes "negative". For higher applied fields, a higher built-in reverse filed is built to keep the cathodic field below $E_{threshold}$.

Effects of Varying the Activator Concentration (N_{a0})

Procedure:

In the simulations for this paper, the number of activators, N_A, is varied between 10^{18} cm^{-3} to $2x10^{19}$ cm^{-3}. Note that the number of traps equals the number of activators.

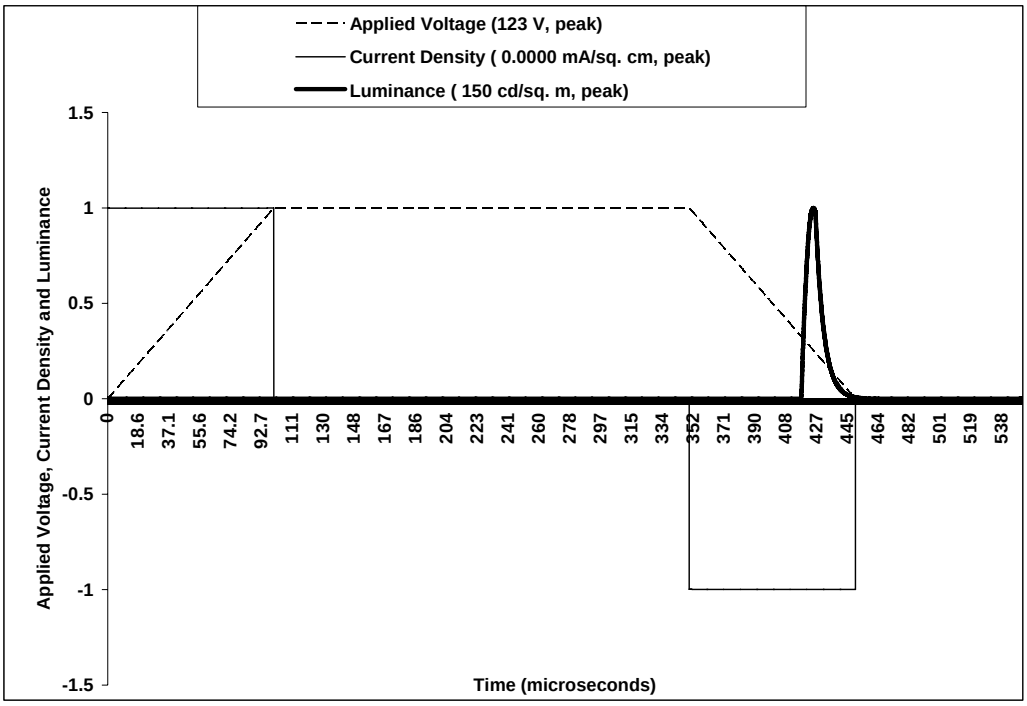

Figure 5.0.1: Simulated voltage, current and luminance waveforms for a SrS:Cu ACTFEL for V_{amp} =123 V for Na_0 = 9.5E10^{18} cm^{-3}

BTE is observed, but no appreciable LE or MTE. Also no appreciable conduction current is observed. Field ionization of activators causes formation of dipoles. When the field drops below the critical threshold, those dipoles collapse. The subsequent relaxation of electrons is seen as emitted luminance in the BTE peak.

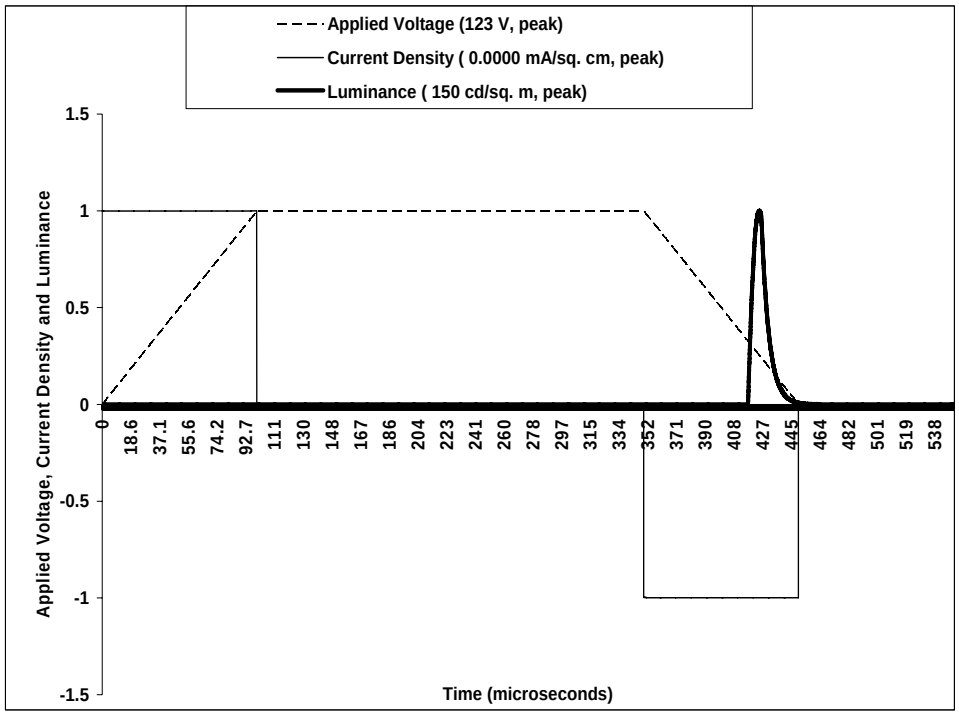

Figure 5.0.2: Simulated voltage, current and luminance waveforms for a SrS:Cu ACTFEL for V_{amp} =123 V for Na_0 = 9.67E10^{18} cm^{-3}

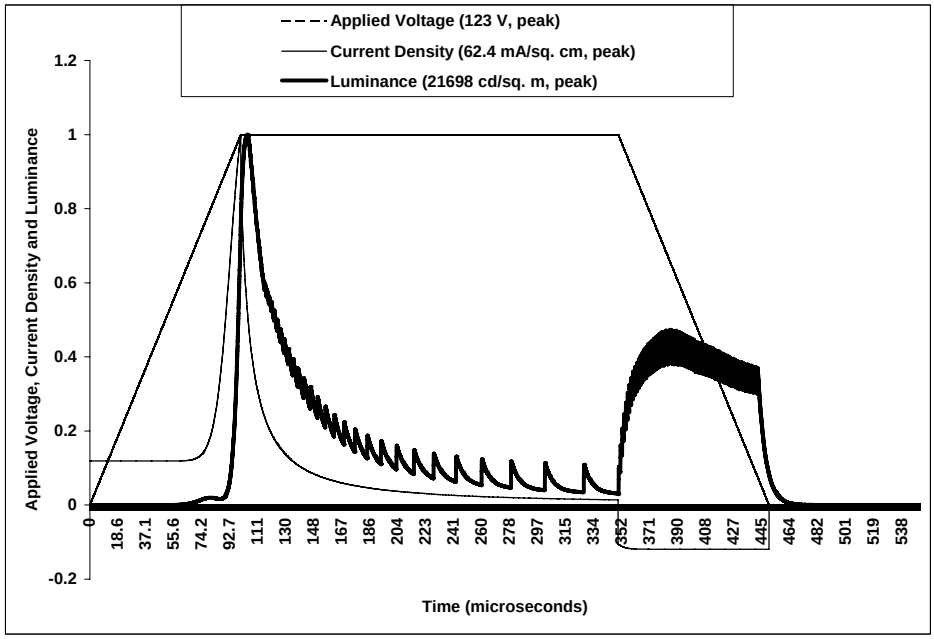

Figure 5.0.3: Simulated voltage, current and luminance waveforms for a SrS:Cu ACTFEL for V_{amp} =123 V for Na_0 = 9.997E10^{18} cm^{-3}.

The highest point of the LE luminance peak (t_{10}) precedes the highest point of the current (t_{11}). Because activator concentration is low, it is partially exhausted of excitable activators. So between t_{10} and t_{11}, even in the presence of increasing flux, there is reduced luminance. Also the MTE peak is higher than the BTE, as in the experimental data. At this voltage the simulated luminance is 50 times greater than the experimental luminance.

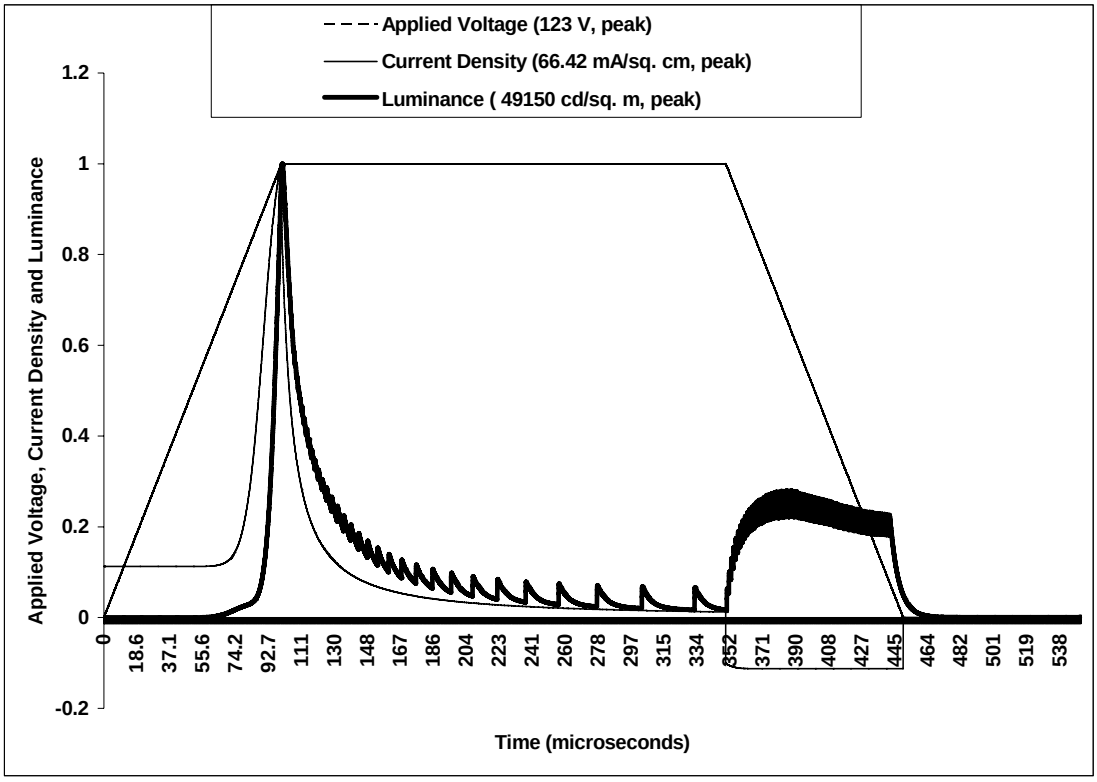

Figure 5.0.4: Simulated voltage, current and luminance waveforms for a SrS:Cu ACTFEL for V_{amp} =123 V for Na_0 = 1.0E10^{19} cm^{-3}

The magnitude of the BTE luminance is large and it exhibits oscillations. Since large number of traps and activators are present in the device, more dipoles are formed. When, these dipoles collapse, more luminance is produced. The reason behind the presence of oscillations is described in Chapter 4.

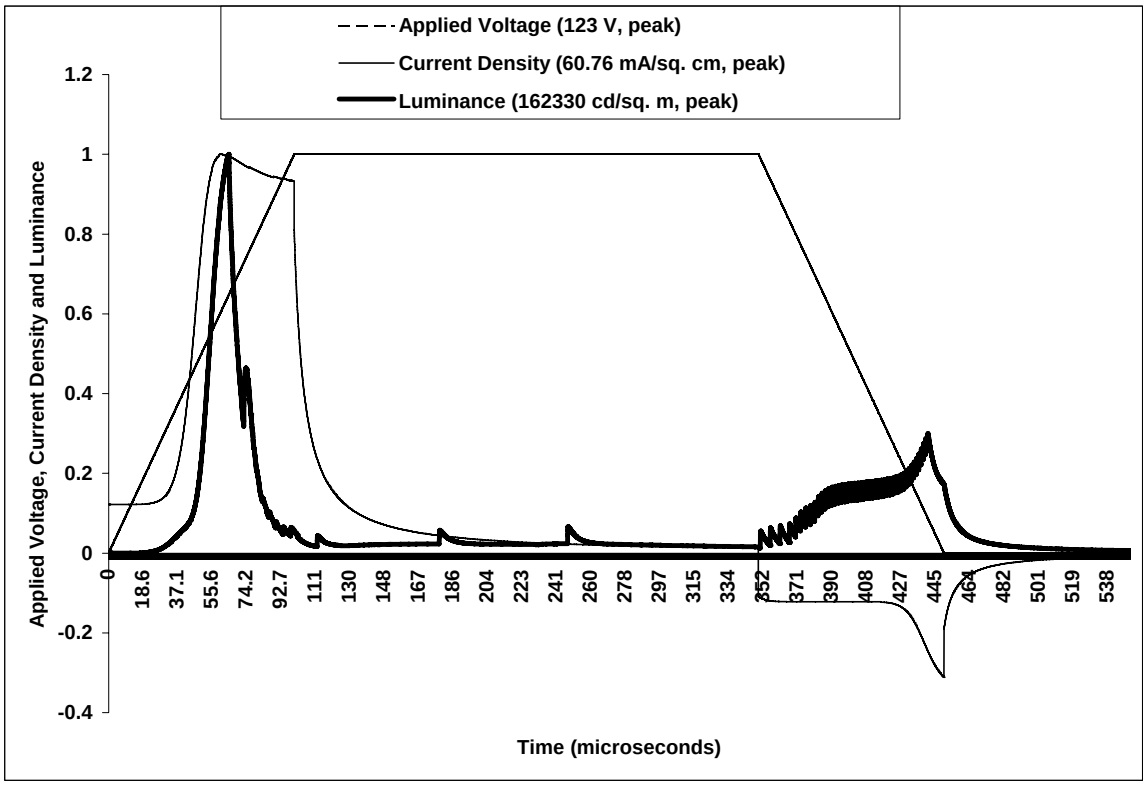

Figure 5.0.5: Simulated voltage, current and luminance waveforms for a SrS:Cu ACTFEL for V_{amp} =123 V for $Na_0 = 1.1E10^{19}$ cm^{-3}

- At $N_{a0} = 10^{19}$ cm^{-3}, only BTE is observed.
- At higher $N_{a0} = 9.67 \text{ X } 10^{18}$ cm^{-3}, luminance peaks before current.
- At still higher $N_{a0} = 10^{19}$ cm^{-3}, luminance peaks after current.
- At still higher $N_{a0} = 2\text{x}10^{19}$ cm^{-3}, BTE vanishes.

For $N_{a0} = 0$, there will not be any emission since there are no activators to excite and relax. Increasing N_{a0} appears to be the best solution, but there is an upper limit. Since activators can get ionized, creating bulk charge and reducing the field near the anode, reduced luminance can occur for higher values of N_{a0}.

Another mechanism that limits the value of N_{a0} is "activator quenching". Upon impact-excitation, the kinetic energy of the electron is transferred to the activator, so that the activator ends up in the excited state. So, electrons need to gain enough kinetic energy before they effectively impact-excite an activator. If the activator concentration is too high, electrons keep colliding with activators before they are "hot" enough, before they have gained enough kinetic energy. When this happens, most of the kinetic energy of the electron is dissipated as heat, so that the electron loses it energy without causing impact-excitation.

Effect of Varying the Depth of the Interface States

Procedure:

Theoretical studies were performed to determine the effect of varying the depth of interface states on the VIL characteristics. The depths of the cathodic and anodic interface states (with respect to the conduction band) were varied over a determined range of values and simulations were performed. The time taken for relaxation from the shallow to the deep interface states was negligible when compared to the time between successive voltage pulses; relaxation time constant from shallow to deep states was taken as 50 ns and the time between successive voltage pulses was taken as 5000μs. As a result, all electrons were present at the deep states at the interfaces when the next voltage pulse was applied to the device.

The depth of the deep interface state (E_{11}), was varied from 0.72 eV to 0.76 eV. The depth of the shallow interface state, E_1, was kept constant at 0.4 eV.

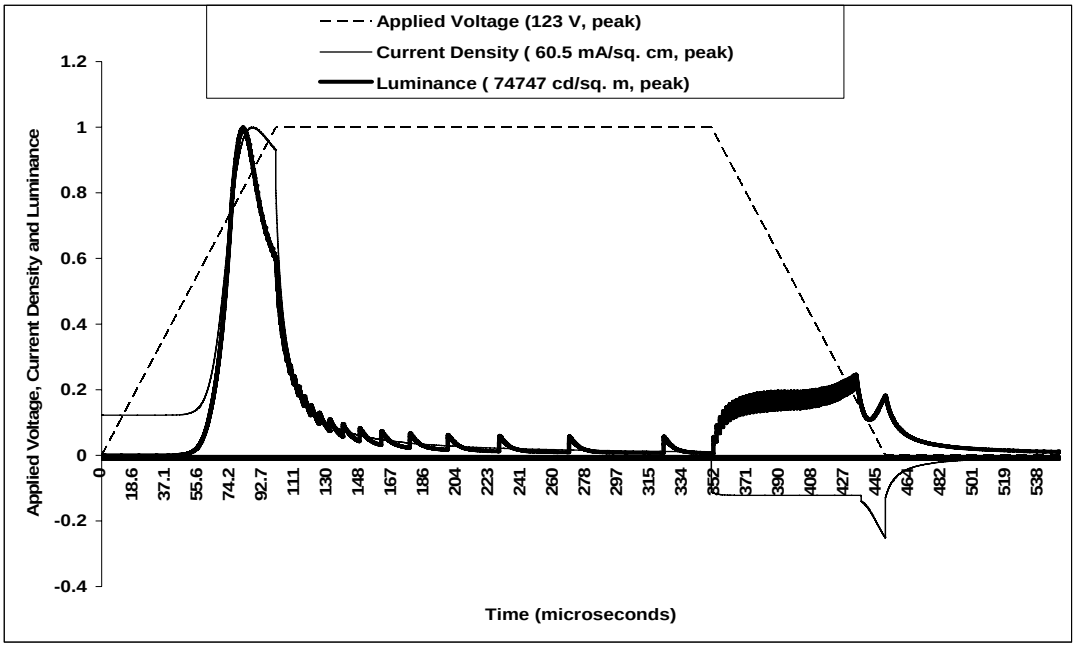

Figure 5.0.6: Simulated voltage, current and luminance waveforms for a SrS:Cu ACTFEL for V_{amp} =123 V for E_{11} = 0.72 eV

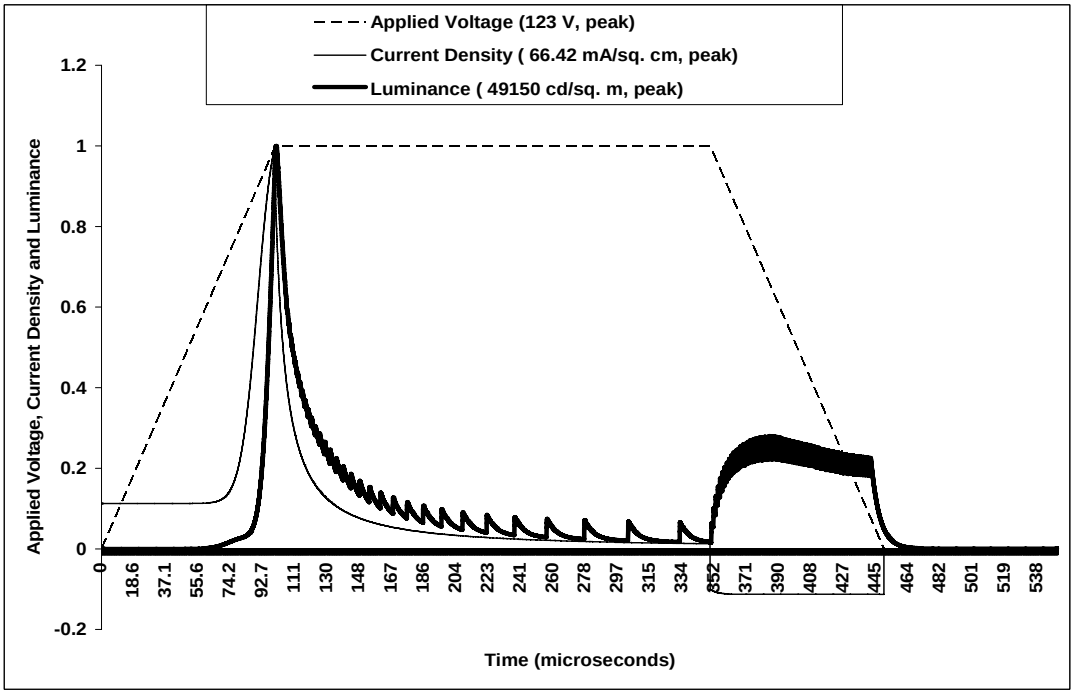

Figure 5.0.7: Simulated voltage, current and luminance waveforms for a SrS:Cu ACTFEL for V_{amp} =123 V for E_{11} = 0.75523 eV

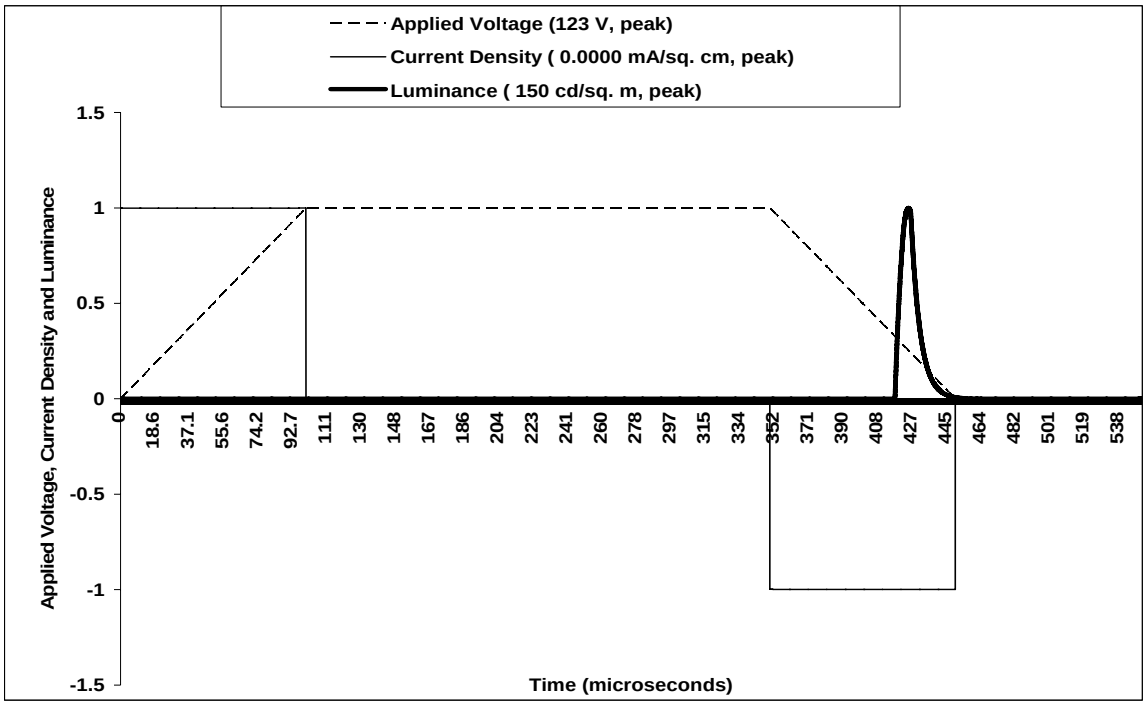

Figure 5.0.8: Simulated voltage, current and luminance waveforms for a SrS:Cu ACTFEL for V_{amp} =123 V for E_{11} = 0.76 eV

As E_{11} increases, the time delay between the current peak and the voltage peak (t_{IV}) diminishes. As E_{11} increases the threshold voltage increases. Conduction current appears later and peaks later in time. Thus t_{IV} decreases as E_{11} is increased until at E_{11} = 0.755233 eV, t_{IV} = 0. t_{IV} remains at zero for higher values of E_{11}. The benchmark was chosen to be at E_{11} = 0.76 eV. The depth of interface states variation can make the current peak shift with respect to the voltage peak.

In our model, based on experimental results, we have assumed that only two levels of interface states exists and that electrons relax from the shallow (E_1) into the deep states (E_{11}). The relaxation time from deep to shallow is short enough (~ few μs) that when a pulse is applied, all the electrons reside in the deep interface states. For this

reason, E_{11} plays an important role in determining the current and luminance characteristics during the first part of the applied pulse.

For high values of E_{11} (0.72 eV) the applied voltage is not strong enough to cause electrons to tunnel from the interface states. As E_{11} decreases and the electrons tunnel out more easily, conduction current and luminance appear. Also, dipoles are formed even when there is not an appreciable amount of impact excitation (E_{11} = 0.72 eV). When E_{11} is within "reach" of the applied field, when conduction current and LE appear, there is also a certain amount of backflow, so that MTE is present whenever LE is. When E_{11} is even shallower (E_{11}= .76 eV), dipole collapse takes place so early in the pulse that LE appears to have a secondary peak, a "shoulder". This is because more charge is transferred; more ionization occurs due to a larger number of electrons flowing across the phosphor and more bulk charge is created. Bulk charge causes a differential between the electric field at the cathodic and anodic sides of the phosphor layer, so that the phosphor section near the anode goes under E_{min} sooner, causing dipoles to collapse earlier.

Effects of Varying the Threshold Electric Field for Dipole Collapse

Procedure:

Simulations were performed to determine the effects of varying the threshold electric field at which dipoles collapse (E_{min}) on the characteristics of the ACTFEL device. E_{min} was varied from 0.3MV/cm to 1.7MV/cm and calculations were performed.

From Fig. 5.0.9, it is observed that the luminance waveform exhibits a jagged waveform between the LE and MTE luminance peaks. This is attributed to the phenomenon of dipole collapse, which is explained as under: Because of spatial and temporal variation of electric field in phosphor, dipoles collapse at different times and in different sections in phosphor. Subsequent relaxation of the electrons within the activator produces luminance. Hence, the BTE peak has a jagged waveform.

It can be noted from the plot that the electric field at the anode has fallen below 0.3 MV/cm at time t1 and hence, the dipoles near the anode begin to collapse at this point. Subsequently, the dipoles in the sections between the cathode and the anode begin to collapse and finally, the dipoles at the cathode collapse.

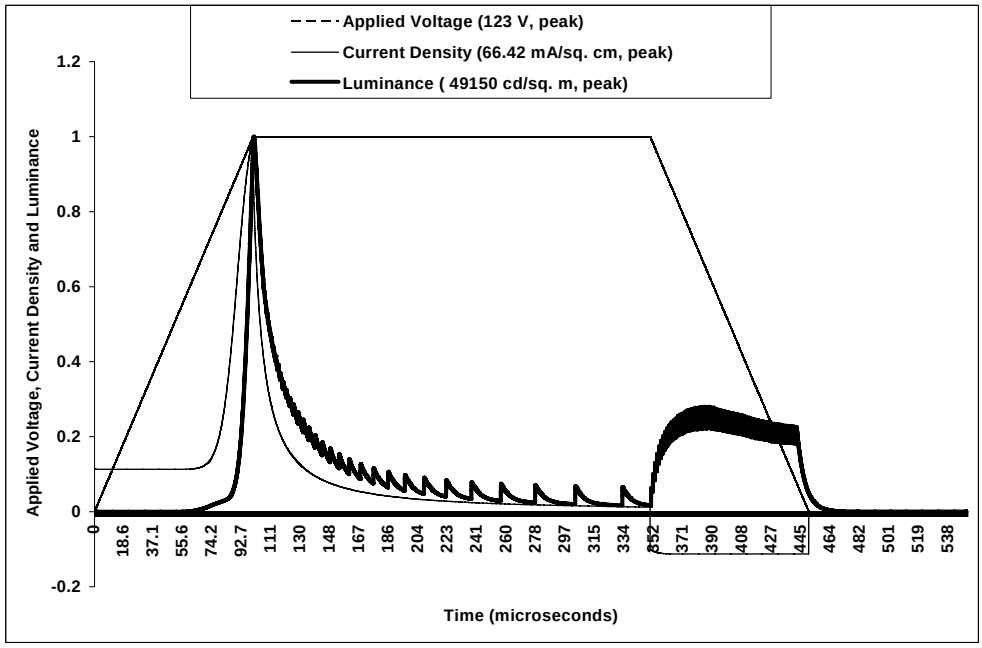

Figure 5.0.9: Simulated voltage, current and luminance waveforms for a SrS:Cu ACTFEL for V_{amp} =123 V for E_{min} = 0.4 MV/cm

Dipoles start collapsing earlier as expected (t2 < t1).

- The BTE luminance exhibits a single peak. Oscillations are observed in this peak.
- In addition to the BTE luminance peak, a number of smaller luminance peaks are observed. Unlike being aggregated close together and near the LE luminance as in Figure, these peaks are spread out much wider and more evenly between the LE and BTE luminance peaks. These smaller peaks appear very close to the LE peak and manifests as a shoulder in the LE luminance.

More dipoles have collapsed by the time BTE arrives. t5< t1 so BTE and MTE separate out E_{min} increases

In addition to the BTE luminance peak, a number of smaller luminance peaks are observed. These peaks occur much earlier than the main LE peak.

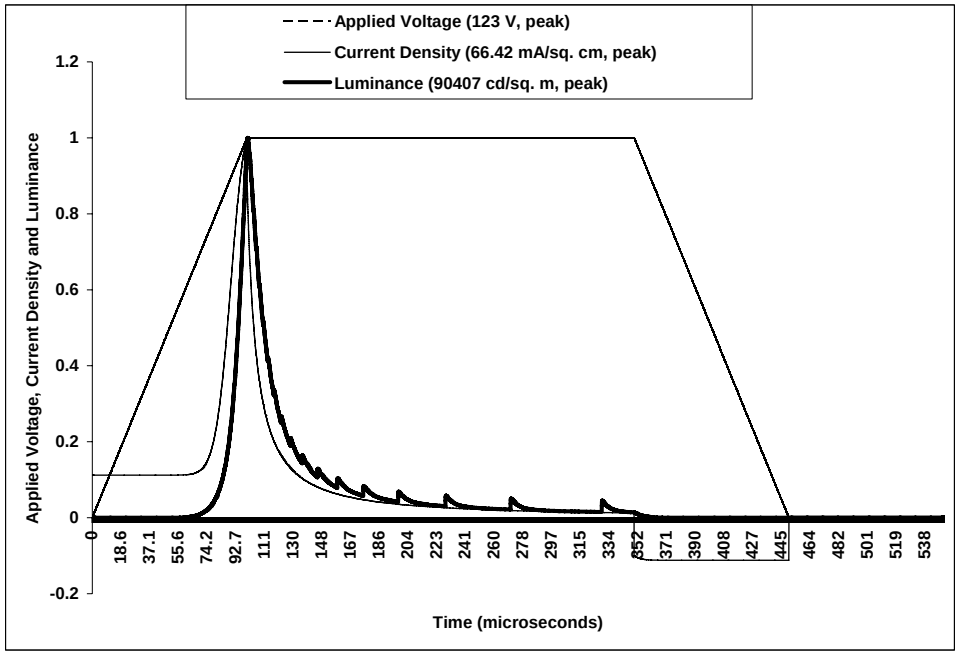

Figure 5.0.10: Simulated voltage, current and luminance waveforms for a SrS:Cu ACTFEL for V_{amp} =123 V for E_{min} = 1.7 MV/cm

BTE is absent. All dipoles have already collapsed before the voltage begins to decrease at the trailing edge. Many SrS:Cu,Ag ACTFEL devices do not show a BTE. Note that the value of E_{min} depends on the physical distance between the activator and its "daughter" trap and the angle between their line-of-sight and the electric field lines.

It was observed that varying the threshold electric field at which dipoles collapse had a significant impact on the BTE luminance (Fig. 5.0.9 and Fig. 5.0.10).

- The peak value of BTE luminance increased as the threshold field for collapse of dipoles was increased until a particular threshold value and then the BTE peak was absent.
- There were fewer oscillations in BTE luminance at higher threshold fields; at very high threshold fields, the oscillations were clearly absent and a single BTE luminance peak was observed.
- The total area under the BTE luminance peak(s) was/were constant.

The observations are reasoned out below:

- The BTE luminance is attributed to collapse of dipoles in the phosphor and subsequent relaxation of the electrons within the activators.
- The time at which these dipoles collapse is determined by the time at which the net electric field in the phosphor goes below the threshold field.
- The electric field varies both in time and space within the phosphor.

- When the field in the phosphor goes below this threshold field, the dipoles in the sections where the net field is less than this threshold field, collapse. The dipoles in the other sections, however, do not collapse.
- Because of spatial and temporal variation of electric field in phosphor, dipoles collapse at different times and in different sections in phosphor. Subsequent relaxation of the electrons within the activator produces luminance. Hence, the BTE peaks have a jagged waveform.
- When the threshold field for dipole collapse is high, there are many sections within the phosphor where field is much below this threshold field. Hence, more dipoles collapse at nearly the same time instant resulting in a single large BTE peak.
- When the threshold field is less, there are many sections in phosphor in which the field is much larger than the threshold field. The dipoles in these sections do not collapse until the field in these sections has fallen below the threshold field. Hence, multiple, though smaller, peaks are seen for lesser threshold fields.
- The total number of dipoles present in the phosphor is, for practical purposes, constant. Hence, the total luminance produced as a result of their collapse and relaxation of the electron within the activator is also a constant. Hence, the area under the BTE luminance peak(s) is/are constant.
- The shoulder in the LE luminance was most predominant when simulations were performed setting the electric field at which the dipoles collapse within the range of 0.5 to 0.6 MV/cm.

In our model, upon electron impact-excitation, activators can lose an electron to the conduction band or to a nearby trap [ ] . When the latter happens, if the electric field is high enough (above E_{min}), the positively charged activator and the negatively charged trap are separated by the electric field by virtue of they opposite charges (if in the right position, otherwise would be brought together). A dipole will be created, which will collapse when the electric field goes below the minimum required to keep activator and trap sufficiently apart. When the electric field goes below E_{min}, the trap gets close to the activator and the electron is transferred to excited energy level of the activator, where it relaxes and emits luminance.

As E_{min} increases, dipole collapse starts later in the pulse. Whit E_{min} = .4 MV/cm exhibiting a "shoulder" in LE. For higher values of E_{min}, dipole collapse practically starts when LE peaks so that the shoulder is not evident for these cases.

As dipole collapse starts earlier, it also ends earlier, as reflected in BTE and MTE merging for (E_{min} = .4 - .6 MV/cm) and later the gap between them increasing as E_{min} increases. One a reasonable time gap between both is reached, the values of BTE and MTE stay at about the same amplitude, independently from E_{min}. For the cases (E_{min} = 0.3 - 0.5 MV/cm) BTE and MTE seem to add up, but for E_{min} = 0.3 MV/cm, the amplitude of the last luminance peak is larger than the amplitudes of BTE and MTE for other cases added together.

Chapter 6

Conclusions

The measured and the simulated peak currents are 72.5 mA/cm^2 (experimental) and 66.42 mA/cm^2 (theoretical) for V_A = 123 V. Experimental and theoretical charge transferred per pulse were 2.75 μC/cm^2 and 2.26 μC/cm^2. Peak experimental and simulated luminance values for V_A = 123 V case were 531 cd/m^2 and 49150 cd/m^2 respectively. Total experimental and simulated luminance values for V_A = 123 V case were 6.2 cd/m^2 and 561.2 cd/cm^2 respectively. Due to internal reflections in the device, losses occurred during luminance collection during measurements. The variation between experimentally observed and simulated luminance can be attributed to the following factors: (i) we have not accounted for the distance an electron must travel (after each impact) to regain enough energy for impact excitation/ionization. (ii) clustering effect of activators and its impact on luminance (iii) quenching because of neighbor defect and (iv) quenching because of concentration. Hence, we have defined a parameter called optical loss factor, k, whose value can be varied according to the specifics of the particular experiment. The optical loss factor takes into account the factors for lower luminance listed above

Simulations of field, current and luminance in SrS: Cu, Ag ACTFEL devices provided new insights into the device and revealed the physical mechanisms by which several “unusual” behaviors in device characteristics are produced. For example, the model predicted that under certain different operating conditions,

- Current in the phosphor can be decreasing during a time interval when the electric field at the cathodic interface is clamped at a constant value (Fig. 4.0.3).
- At a "low" activator concentration value of 9.5×10^{18} cm^{-3}, the luminance waveform exhibits the first trailing edge pulse (BTE), but no leading edge (LE) and MTE pulses (as in Fig. 5.0.8). At a higher activator concentration value of 9.997×10^{18} cm^{-3}, the luminance waveform exhibits all three pulses, the LE, the BTE and the MTE (Fig. 5.0.10). At the leading edge, luminance peaks before current. At yet higher activator concentration value of 10^{19} cm^{-3}, the luminance waveform exhibits all three pulses (Fig. 5.0.11), but now, at the leading edge, luminance peaks after current.

In summary, the model is able to predict all "unusual" features in the response of the SrS:Cu,Ag ACTFEL device. Furthermore, the general model [1]-[2] used in this investigation can be applied to ACTFEL devices (such as yellow-emitting ZnS:Mn devices), other than SrS:Cu,Ag, as simpler, special cases.

The depth of interface states variation can make the current peak shift with respect to the voltage peak. The presence of BTE depends on the value of E_{min}.

We have used the model presented in [1] to study the behavior of ACTFEL devices as several important parameters (voltage amplitude $V_{amp,}$ activator concentration

N_{a0}, dipole collapse field E_{min}, interface states energy level E_{11} and dipole formation probability fnew3 affect the device behavior.

The “shoulder” in LE, can be thought of as an early BTE and can appear as any of the parameters studied here (voltage amplitude, dipole formation probability, activator concentration, interface state energy level and dipole collapse field) is varied.

Future Work

This thesis has brought out some interesting characteristics of the ACTFEL devices and shows the qualitative and quantitative match between theory and experiments. In the future, we can do experiments with change in temperature using the cryostat. These experiments, when matched with the simulations, would be an area for future work. Another area of future work could be doing transient measurements and time resolved spectroscopy.

References

[1] V. P. Singh, P. Sivakumar, A. Aguilera, D. C. Morton and E. Forsythe, "An Analytical Model For Electron Transport and Luminance in SrS:Cu,Ag ACTFEL Display Devices", IEEE Transactions on Electron Devices, vol. 51, No. 3, pp. 357-363, (2004).

[2] V. P. Singh, A. Aguilera, A. Garcia and D. C. Morton, "Modeling of Electron Transport and Luminance in SrS:Cu, Ag ACTFEL Display Devices", IEEE Transactions on Electron Devices, Vol. 48, No. 10, pp. 2242-2248 (2001).

[3] S. S. Sun, E. Dickey, J. Kane and P. Yokum, "A Bright and Efficient New Blue TFEL Phosphor", Conf. Rec. '97 IDRC (International Displays Research Conference), pp. 301-305, (1997).

[4] W. Tong, Y.B. Xim, W. Park, and C.J. Summers, "Mn pinning effect in SrS thin-film electroluminescent phosphors", Appl. Phys. Lett., 74, pp. 1379, (1999).

[5] P.D. Keir, J. F. Wager, B.L. Clark, D.Li and K.A. Kezler, "Alkali metal co-activators in SrS: Cu,F thin-film electroluminescent devices", Appl. Phys. Lett., 75, pp. 1398, (1999).

[6] D. Wauters, D. Poelman, R.L. Van Meirhaeghe, F. Cardon, "Optical characterization of SrS:Cu and SrS:Cu,Ag EL devices", J. of Luminescence, 91, pp. 1-6 (2000).

[7] N.A. Vlasenko, Y.A. Kononets, Yu.V. Kopytko, E.Soininen, S.–S. Sun, "Temperature dependence of characteristics of SrS:Cu(Ag) thin-film electroluminescent devices beyond room temperature", J. Crystal growth, 216, pp. 245-248, (2000).

[8] D. C. Morton, E. Forsythe, S.-S. Sun, M. C. Wood, M. H. Ervin and C. Kirchner, "Thermally stimulated luminescence of SrS:Cu thin films", Appl. Physics Lett., vol. 78, No. 10, pp. 1400-1402, (2001).

[9] A. Aguilera, V. P. Singh and D.C. Morton, "Electron Energy Distribution at the Insulator-Semiconductor Interface in A.C. Thin Film Electroluminescent Display Devices", IEEE Trans. Electron Devices, vol. 41, No. 8, pp. 1357-1363, (1994).

[10] M. Peters, S. Nishimura, M. Murayama, K. Ohmi, S. Tanaka, H. Kobayashi, "Activator ionization and deep level ionization in SrS:Ce ac thin-film electroluminescent devices", J. Appl. Phys., vol. 86, No. 12, pp. 7071-7076, (1999).

[11] P. Sivakumar, "Analysis of electron transport and luminance in SrS based blue emitting A. C. thin film electroluminescent devices", M. S. Thesis, University of Kentucky, 2003.

[12] C.J. Summers, B. K. Wagner, W. Tong, W. Park, M. Chaichimansour and Y. B. Xin, "Recent progress in the development of full color SrS-based electroluminescent phosphors", J. Crystal growth, vol. 214-215, pp. 918-925, (2000).

[13] C. N. King, “Electroluminescent Displays”, Seminar Lecture Notes, SID-96, Soc. For Information Display, San Diego, pp. M-9, 1-36, (1996).

[14] B. Huttl, U. Troppenz, K.O. Velthaus, C. R. Rhonda, R. H. Mauch, “Luminescence properties of SrS:Ce^{+3}”, J. Appl. Physics, vol. 78, pp. 7282, (1995).

Appendix 1

Mathematical Model for Opto-Electronic Processes in SrS ACTFEL devices

The comprehensive mathematical model for the opto-electronic processes in generic ACTFEL devices (whose structure is as shown in Fig. 3.0.2) can be found here [2]. The equations are reproduced here for reference.

Tunneling from Interfaces

$$f = f_{OS} n_{SC} P_{SC}(E) + f_{OD} n_{DC} P_{DC}(E) \tag{1}$$

$$P_{SC}(E) = a\left(\frac{m}{m^*}\right)^{\frac{1}{8}} E_{SC}^{\frac{5}{8}} E^{\frac{1}{4}} \exp\frac{-b\left(m^*/m\right)^{\frac{1}{2}} E_{SC}^{\frac{3}{2}}}{E} \tag{2}$$

$$P_{DC}(E) = a\left(\frac{m}{m^*}\right)^{\frac{1}{8}} E_{DC}^{\frac{5}{8}} E^{\frac{1}{4}} \exp\frac{-b\left(m^*/m\right)^{\frac{1}{2}} E_{DC}^{\frac{3}{2}}}{E} \tag{3}$$

Impact Excitation of an Electron from E_{AL} to E_{AH}

$$R_1 = \alpha \cdot f \cdot f_1(E) \cdot u(x,t) \tag{4}$$

$\alpha = \pi \cdot r^2$

$$f_1(E) = \begin{cases} 0 & for \quad 0 < E \le .3\frac{MV}{cm} \\ \left(\dfrac{E - .3\times10^6}{.65\times10^6 - .3\times10^6}\right)^2 & for \quad 0.3\frac{MV}{cm} < E \le .65\frac{MV}{cm} \\ 1 - (f_2(E) + f_2^I(E)) & for \quad 0.65\frac{MV}{cm} < E \le 1.1\frac{MV}{cm} \\ 0 & for \quad 1.1\frac{MV}{cm} < E \end{cases} \tag{5}$$

$$f_2(E)=\begin{cases}0 & 0<E\le .65\frac{MV}{cm}\\ .33\left(\dfrac{E-.65\times10^6}{1.1\times10^6-.65\times10^6}\right)^2 & 0.65\frac{MV}{cm}<E\le 1.1\frac{MV}{cm}\\ .33 & 1.1\frac{MV}{cm}<E\end{cases} \tag{6}$$

Dipole Creation (ionized activator- nearby trap)

$$R_{2A}=\begin{cases}u(x,t)\cdot f\cdot f_3(E)\cdot f_2(E)\cdot\pi\cdot R^2 & u(x,t)<<p_T\\ p_T\cdot f\cdot f_2(E)\cdot\pi\cdot R^2 & u(x,t)>>p_T\end{cases}$$

(7)

$$R_{2B}=\begin{cases}u(x,t)\cdot P_{EALE1} & u(x,t)<<p_T\\ p_T\cdot P_{EALE1} & u(x,t)>>p_T\end{cases} \tag{8}$$

$$P_{EALE1}(E)=a\left(\frac{m}{m^*}\right)^{\frac{1}{8}}\Delta E_{EALE1}^{\frac{5}{8}}E^{\frac{1}{4}}\exp\frac{-b\left(m^*/m\right)^{\frac{1}{2}}\Delta E_{EALE1}^{\frac{3}{2}}}{E} \tag{9}$$

$R_2 = R_{2A} + R_{2B}$

$$R_{12A}=\begin{cases}e(x,t)\cdot f\ \cdot f_3^I(E)f_2^I(E)\cdot\pi\cdot R^2 & e(x,t)<<p_T\\ p_T\cdot f\cdot f_3^I(E)f_2^I(E)\cdot\pi\cdot R^2 & e(x,t)>>p_T\end{cases} \tag{10}$$

$$R_{12B}=\begin{cases}e(x,t)\cdot P_{EAHE1} & e(x,t)\le p_T\\ p_T\cdot P_{EAHE1} & e(x,t)>p_T\end{cases} \tag{11}$$

$$P_{EAHE1}(E)=a\left(\frac{m}{m^*}\right)^{\frac{1}{8}}\Delta E_{EAHE1}^{\frac{5}{8}}E^{\frac{1}{4}}\exp\frac{-b\left(m^*/m\right)^{\frac{1}{2}}\Delta E_{EAHE1}^{\frac{3}{2}}}{E} \tag{12}$$

Impact Ionization to Conduction Band

$R_3 = (R_3)_{E_{AL}} + (R_3)_{E_{AH}}$

(13)

or $R_3 = (f\cdot f_2(E)\cdot u(x,t)\cdot[1-f_3(E)]+ f\cdot f_2^I(E)\cdot e(x,t)\cdot[1-f_3^I(E)])\pi R^2$ (14)

Activator Relaxation

$$R_4 = e(x,t) \cdot \gamma \tag{15}$$

Dipole Collapse

$$R_5 = \frac{n_{t2} \cdot \sigma_5(E)}{\tau_d} \tag{16}$$

$$\sigma_5(E) = \begin{cases} 1 & E \le E_{\min} \\ 0 & E > E_{\min} \end{cases} \tag{17}$$

Charge Transfer from the Trap level to the Conduction Band

$$R_6 = n_{t2} P_{E1EC} \tag{18}$$

$$P_{E1EC}(E) = a\left(\frac{m}{m^*}\right)^{\frac{1}{8}} \Delta E_{E1EC}^{\frac{5}{8}} E^{\frac{1}{4}} \exp\frac{-b\left(m^* \diagup m\right)^{\frac{1}{2}} \Delta E_{E1}^{\frac{3}{2}}}{E} \tag{19}$$

Electron Relaxation from the Conduction Band to Bulk Traps

$$R_7 = f \cdot p_T \cdot S_{nt} \frac{v_{TH}}{v_{SAT}} \tag{20}$$

Charge Transfer between the Ionized Activators and Shallow Anodic Interface States

$$R_8 = \begin{cases} \dfrac{[u_0 - u(x,t) - e(x,t)]\sigma_8(E)u(t-t_8)}{\Delta t} & for \quad [u_0 - u(x,t) - e(x,t)] \le n_{AIS} \\ \dfrac{n_{AIS}\sigma_8(E)u(t-t_8)}{\Delta t} & for \quad [u_0 - u(x,t) - e(x,t)] > n_{AIS} \end{cases} \tag{21}$$

$$u(t-t_8) = \begin{cases} 0 & t \le t_8 \\ 1 & t > t_8 \end{cases} \tag{22}$$

Rate of change of electron population at the lower energy level (E_{AL}) of the copper activator in the phosphor layer

$$\frac{du(i)}{dt} = -R_1 - R_2 - R_3 + R_4 \tag{23}$$

Rate of change of electron population at the upper energy level (E_{AH}) of the activator in the phosphor layer

$$\frac{de(i)}{dt} = R_1 - R_4 + R_5 - R_6 + R_7 - R_{12} \tag{24}$$

Rate of change of electron population at the bulk traps is given by

$$\frac{dn_{t2}(i)}{dt} = R_2 + R_{12} - R_5 \tag{25}$$

Flux variation

For the purpose of numerical analysis, the phosphor layer is divided into n subsections of width W_X each. Flux variation from one subsection (i-1) to the adjacent subsection (i) can be expressed as

$$f(i) = f(i-1) + W_X\left[R_3 + R_6 - R_7\right] \tag{26}$$

where f(i) is the electron flux in the conduction band of the i^{th} subsection of the phosphor layer.

Luminance output of the i^{th} subsection of phosphor layer during the simulation time interval Δt

$$L(i,t) = W_x \cdot e(x,t) \cdot \Delta t \cdot \gamma \tag{27}$$

$$\gamma = 1/\tau \tag{28}$$

Total luminance

$$L(t) = \sum_{i=1}^{n} L(i,t) \tag{29}$$

These equations are used to calculate the field, current and luminance in the device. For computing the local electric field, the method reported in [12] was used.

Appendix 2

Program

```
/*****************************************************************

  Title:  Actfel.c

  Using 2 interface states
  Author: Dharmashankar Rajagopalan

*****************************************************************/

    # include <stdio.h>
    # include <stdlib.h>
    # include <math.h>
    # include "constants.h"  /* All the constants are defined here */
    # include "variables.h"  /* All the global variables are declared here */

    void init(void);
    void exchange(void);
    void driver(void);
    void anodic_interface(void);
    void write_scaled_file(void);
    void constants(void);
    void cathodic_tunneling(void);
    void bulk_phosphor(void);
    void shallow_states(void);
    void cathodic_interface(void);
    void anodic_interface(void);
    void anodic_tunneling(void);

    int main (int argc, const char * argv[]) {
        Infofile = fopen("info.txt","w+");
        Scaledfile = fopen("vil.xls","w+");
        FluxFile = fopen("condflux.xls","w+");
        flux_direction = 0;

        init();
        j = 1;
        z = 1;
        while( z <= NO_OF_PULSES)
        {
                set_tunnel = 0;
```

```
                fld_tunnel = 0;
                t = 0;

                printf(" Pulse number %d is running currently \n ", z );
                if( z != 1)
                        exchange();

                driver();
                anodic_interface();
                write_scaled_file();

                if (z==199)
                {
                //fprintf(Infofile,"Pulse Number: %d\n\n",z);
                fprintf(Infofile,"Applied Voltage = %f V\n\n\n",Vs);
                fprintf(Infofile,"Maximum Luminance = %.20lf
W/sq.m\n\n\n",max_lum*K*10000);

                fprintf(Infofile,"Luminance per period = %.20lf W/sq.
m\n\n\n",tot_luminance*K*10000*50E-9/5000E-6);
                fprintf(Infofile,"Maximum Current = %.20lf A/sq.
cm\n\n\n",max_flux*1.6E-19);

                fprintf(Infofile,"Total Charge = %.20lf A/sq. cm\n\n\n",totalflux*1.6E-
19*50E-9);

                fprintf(Infofile,"Maximum Cathodic Electric Field = %f
V/cm\n\n\n",max_e_cathode);

                fprintf(Infofile,"Maximum Anodic Electric Field = %f
V/cm\n\n\n",max_e_anode);

                }
                ++z;

        }

        fclose(Scaledfile);

        fclose(Infofile);

        fclose(FluxFile);

       return 0;
    }
```

```
void write_scaled_file(void)
{
      max_lum = Lum[0];
      tot_luminance = 0;
   totalflux = 0;

      for(run_t = 0;run_t<t+1;run_t++)
      {
            if (max_lum<Lum[run_t])
            {
                  max_lum = Lum[run_t];
            }
            tot_luminance = tot_luminance + Lum[run_t];
      }

      max_e_cathode = e_cathode[0];
      for(run_t = 0;run_t<t+1;run_t++)
      {
            if (max_e_cathode<e_cathode[run_t])
            {
                  max_e_cathode = e_cathode[run_t];
            }
      }

      for(run_t = 0;run_t<t+1;run_t++)
      {
            e_cathode[run_t] = e_cathode[run_t]/max_e_cathode;
      }

      max_e_anode = e_anode[0];

      for(run_t = 0;run_t<t+1;run_t++)
      {
            if (max_e_anode<e_anode[run_t])
            {
                  max_e_anode = e_anode[run_t];
            }
      }

      for(run_t = 0;run_t<t+1;run_t++)
      {
            e_anode[run_t] = e_anode[run_t]/max_e_anode;
      }
```

```
for(run_t = 0;run_t<t+1;run_t++)
{
	Lum[run_t] = Lum[run_t]/max_lum;
}

max_v = Vol[0];

for(run_t = 0;run_t<t+1;run_t++)
{
	if (max_v<Vol[run_t])
	{
		max_v = Vol[run_t];
	}
}

for(run_t = 0;run_t<t+1;run_t++)
{
	Vol[run_t] = Vol[run_t]/max_v;
}


max_flux = Flu[0];

for(run_t = 0;run_t<t+1;run_t++)
{
	if (max_flux<Flu[run_t])
	{
		max_flux = Flu[run_t];
	}
}

for(run_t = 0;run_t<t+1;run_t++)
{
	totalflux = totalflux + Flu[run_t];

	Flu[run_t] = Flu[run_t]/max_flux;
}

max_flux_disp = 0;


for(run_t = 1;run_t<t+1;run_t++)
{
	flux_disp = ((6.8624E-9)*((Vol[run_t]-
Vol[run_t+1]))*max_v)/(q*delta_T);
```

```
                if (max_flux_disp < flux_disp)
                {
                        max_flux_disp = flux_disp;
                }
        }

        max_flux_disp = max_flux_disp/max_flux;

        if ((z==199)|(z==200))
        {
                for (run_t = 1;run_t<=1000;run_t++)
                {
                        fprintf(Scaledfile,"%.5lf        %.5lf   %.5lf   %.5lf
        %.5lf\n",0.0,0.0,0.0,0.0,0.0);
                }

                for (run_t=1;run_t<(t+1001);run_t++)
                {
                        flux_disp = ((6.8624E-9)*((Vol[run_t]-
Vol[run_t+1]))*max_v)/(q*delta_T);
                        if ((z % 2)!= 0)
                        {
                                if (run_t < flux_point)
                                {
                                        tot_flux_unscaled =
Flu[run_t]+(flux_disp/max_flux);

                                        tot_flux_scaled =
tot_flux_unscaled/(1+max_flux_disp);

                                        fprintf(Scaledfile,"%.5lf        %.5lf   %.5lf   %.5lf
        %.5lf\n",Vol[run_t-1],tot_flux_scaled,Lum[run_t], e_cathode[run_t],
e_anode[run_t]);

                                        fprintf(FluxFile,"%.10lf\n",Flu[run_t]);

                                }

                                if (run_t > flux_point)
                                {
                                        tot_flux_unscaled = -
Flu[run_t]+(flux_disp/max_flux);

                                        tot_flux_scaled =
tot_flux_unscaled/(1+max_flux_disp);
```

```
                                        fprintf(Scaledfile,"%.5lf    %.5lf  %.5lf  %.5lf
    %.5lf\n",Vol[run_t],tot_flux_scaled,Lum[run_t], e_cathode[run_t],
e_anode[run_t]);

                                        fprintf(FluxFile,"%.10lf\n",-Flu[run_t]);
                                }
                        }
                        else
                        {

                                if (run_t < flux_point)
                                {
                                        tot_flux_unscaled =
Flu[run_t]+(flux_disp/max_flux);

                                        tot_flux_scaled =
tot_flux_unscaled/(1+max_flux_disp);

                                        fprintf(Scaledfile,"%.5lf    %.5lf  %.5lf  %.5lf
    %.5lf\n",-Vol[run_t],-tot_flux_scaled,Lum[run_t], e_cathode[run_t],
e_anode[run_t]);

                                        fprintf(FluxFile,"%.10lf\n",Flu[run_t]);
                                }

                                if (run_t > flux_point)
                                {
                                        tot_flux_unscaled = -
Flu[run_t]+(flux_disp/max_flux);

                                        tot_flux_scaled =
tot_flux_unscaled/(1+max_flux_disp);

                                        fprintf(Scaledfile,"%.5lf    %.5lf  %.5lf  %.5lf
    %.5lf\n",-Vol[run_t],-tot_flux_scaled,Lum[run_t], e_cathode[run_t],
e_anode[run_t]);

                                        fprintf(FluxFile,"%.10lf\n",-Flu[run_t]);
                                }
                        }
                }
        }
    }

    void driver(void) {
        int k ;
```

```
    Vapp = 0;
    for(t_i=1;t_i<=(2*Ts);++t_i) {
            /* WRD: ctr_i is never referenced! */
/*          ctr_i = t_i; */
            if( t_i <= RISE_TIME )              {
                    Vapp += (Vs/RISE_TIME);
            }
            if((t_i>RISE_TIME) && (t_i<=FALL_TIME))
            {
                    Vapp=Vs;
            }

            if( (t_i > FALL_TIME) && (t_i <= Ts) ) {
                    Vapp -= (Vs/(Ts-FALL_TIME));
            }

            constants();
            cathodic_tunneling();
            bulk_phosphor();

            if (z==199)
            {
                    Lt = 0;
                    nahct = 0;
                    for(k = 1; k <= n; ++k) {
                            Lt += (phos[k].Lit);
                            nahct = nahct + phos[k].nah;
                    }
                    e_cathode[t] = phos[1].c3;
                    e_anode[t] = phos[n].c3;
                    Lum[t] = Lt;
                    Vol[t] = Vapp;
                    Flu[t] = phos[n].Fn;
                    t++;
            }
            ++j;
    }

    return;
}


void init (void)
{
    int k;
```

```
    for ( k=1; k<=n; ++k )
    {
            phos[k].nah = 0;
            phos[k].nt2 = 0;
            phos[k].nal = Nao-phos[k].nt2;
            phos[k].Fn = 0;
            phos[k].condnband = 0;
    }

    phos[0].Fn = 0;
    nc1 = 0.0*Neq;
    nc11 = Neq;
    na1 = 0.0*Neq;
    na11 = Neq;
    flux_disp = 0.6863E17;

      return;
}

void cathodic_tunneling(void)
{
    double fld;
    double Pc1,Pc11,d1,d11;
    double f1,f11;

    fld = phos[1].c3;

    if(fld<0)
      {
           phos[0].Fn = 0;
    }
    else
    {
            register double quot; /* a temporary quotient */
            register double cc; /* a temporary constant */


            cc = (-b1) / (sqrt(m/m_star) * fld);
            d1 = cc * pow(E1, 1.5);
            d11 = cc * pow(E11,1.5);
            cc =  a1 * pow(m/m_star, 0.125) * pow(fld, 0.25);
            Pc1 = cc * pow( E1, 0.625) * exp(d1);
            Pc11= cc * pow( E11, 0.625) * exp(d11);
            f1 = nc1*Pc1;
            f11 = nc11*Pc11;
```

```
            quot = nc1 * (1.0/delta_T);
            f1 = (f1 > quot) ? quot : f1;

            quot = nc11 * (1.0/delta_T);
            f11 = (f11> quot) ? quot : f11;

            if(f1<0)
            {
                    printf("f1<0 => Error in cathodic interface \n");
                    exit(0);
            }

            if(f11<0)
            {
                    printf("f11<0 => Error in cathodic interface \n");
                    exit(0);
            }

            nc1 = nc1 - (f1 * delta_T);
            if (nc1<0)
            {
                    f1 = f1 + nc1 * (1.0/delta_T);
                    nc1 = 0;
            }

            nc11 = nc11 - (f11*delta_T);
            if (nc11<0)
            {
                    f1 = f1 + nc11 * (1.0/delta_T);
                    nc11 = 0;
            }
            phos[0].Fn = f1 + f11;
            if (set_tunnel==0)
            {
                    if ((f1+f11)>1E16)
                    {
                            fld_tunnel = phos[1].c3;
                            set_tunnel = 1;
                    }
            }
    }

    return;
}
```

```
void forward_phosphor(void)
{
   register double fld;
   register double dnaldt, dnal, dnahdt, dnt2dt, dnah ;
   register double sigma8;
   register double Prob3;/* a temporary variable refactored from Prob and Prob2;n
                          * it could probably have a better name, but I don't know
what
                          * it is for...
                          */
   /* WRD: converted these variables from arrays to scalars.
    * because the array was never used as an array
    */
   register double R1, R2, R2A, R3, R4, R5, R8, R9, R12, R12A, R13;

   int k;

   for (k=1;k<=n;k++)
   {
         fld = phos[k].c3;
         fnew1 = 0.0;
         fnew2 = 0.0;
         fprimenew2 = 0.0;

         fld = fabs(fld);
         /* WRD: redundant (set above) */
         /* if (fld<(0.25E6))
          * fnew1, fnew2, and fprimenew2 should be zero, and were already
          * set to zero above.
          */
         if ((fld>(0.25E6))&&(fld<(0.55E6)))
         {
               /* WRD: fnew1 >= 0 because it is a square (and fld > 0.25E6) */
               fnew1 = (fld*fld - fld*(2.0*0.25E6) +
(0.25E6*0.25E6))*(1.0/(0.35E6*0.35E6));
         }
         else if ((fld>(0.55E6))&&(fld<(1.0E6)))
         {
               register double ff;
               /* WRD: what if (fld == 0.55E6) precisely? */
               ff = (fld*fld - fld * (2.0 * 0.55E6) + (0.55E6 *
0.55E6))*(1.0/(0.35E6 * 0.35E6));
               /* fnew2 >= 0 and fprimenew2 >=0 because ff is a square (and fld
> 0.55E6) */
               fnew2 = 0.33 * ff;
```

```
                        fprimenew2 = 0.67 * ff;
                        fnew1 = 1.0 - (fnew2+fprimenew2);
                        if (fnew1<0.0)
                        {
                                fnew1=0.0;
                        }
                }
                else if (fld > 1.0E6)
                {
                        /* WRD: what if (fld == 1.0E6) precisely? */
                        fnew2 = 0.33;
                        fprimenew2 = 0.67;
                }
                phos[k].Lit = phos[k].nah * (B * Wx / TAU2) ;
                phos[k].actcharge = Nao-phos[k].nal-phos[k].nah;
                Prob3 = 3.14*radiu*radiu*(phos[k-1].Fn);
                R1 = Prob3*fnew1*phos[k].nal;
                R4 = phos[k].nah * (1.0/TAU2);
                phos[k].nt2 = (phos[k].nt2 > Nt2) ? Nt2 : phos[k].nt2;
                pt = Nt2-phos[k].nt2;
                R2A = Prob3*fnew2*fnew3;
                R2 = R2A * ((phos[k].nal <= pt) ? phos[k].nal : pt);
                R12A = Prob3*fprimenew2*fprimenew3;
                R12 = R12A * ((phos[k].nah <= pt) ? phos[k].nah : pt);
                sigma8 =  (fld > 400000.0) ? 0.0 : (1.0/(delta_Tdipole));
                R8 = sigma8 * ((phos[k].nt2 <= (Nao-phos[k].nal-phos[k].nah-
phos[k].condnband)) ?
                                phos[k].nt2 : (Nao-phos[k].nal-phos[k].nah-
phos[k].condnband));
                R3 = Prob3*fnew2*(1 - fnew3) * phos[k].nal;
                R13 = Prob3*fprimenew2*(1-fprimenew3)*phos[k].nah;
                R5 = 0.0;
                R9 = 0.0;
        //      dtc = (-b1) * pow( ( m/m_star), -0.5) * pow(Etc, 1.5) * (1/fld);
        //      Ptc = a1 * pow( ( m/m_star), 0.125) * pow( Etc, 0.625) * pow(fld, 0.25)
*exp(dtc);
                dnaldt = R4 - R1 - R2 - R3;
                dnahdt = R1 - R4 + R8 - R12 + R9 - R13 + R5;
                dnt2dt = R12 - R8 + R2;
                phos[k].Fn = phos[k-1].Fn + (R3 + R13 - R9 -R5)*Wx;
                dnt2 = dnt2dt * delta_T;
                phos[k].nt2 += dnt2;
                dnal = dnaldt * delta_T;
                phos[k].nal += dnal;
                dnah = dnahdt * delta_T;
                phos[k].nah += dnah;
```

```
                phos[k].condnband = (R3 + R13 - R9)*delta_T;
                total_charge = total_charge+(Nao-
(phos[k].nal+phos[k].nah+phos[k].nt2))*Wx;
        }
        flux_direction = 0;
        anodic_interface();
    }

    void backward_phosphor(void)
    {
        register double fld;
        register double dnaldt, dnal, dnahdt, dnt2dt, dnah ;
        register double sigma8;
        register double Prob3;/* a temporary variable refactored from Prob and Prob2;n
                                * it could probably have a better name, but I don't know
what
                                * it is for...
                                */
        /* WRD: converted these variables from arrays to scalars.
         * because the array was never used as an array
         */
        register double R1, R2, R2A, R3, R4, R5, R8, R9, R12, R12A, R13;

        int k;

        phos[n+1].Fn = phos[n].Fn;
        for (k=n;k>=1;k--)
        {
                fld = phos[k].c3;
                fnew1 = 0.0;
                fnew2 = 0.0;
                fprimenew2 = 0.0;

                fld = fabs(fld);
                if ((fld>(0.25E6))&&(fld<(0.55E6)))
                {
                        fnew1 = (fld*fld - fld*(2.0*0.25E6) +
(0.25E6*0.25E6))*(1.0/(0.35E6*0.35E6));
                }
                else if ((fld>(0.55E6))&&(fld<(1.0E6)))
                {
                        register double ff;

                        ff = (fld*fld - fld * (2.0 * 0.55E6) + (0.55E6 *
0.55E6))*(1.0/(0.35E6 * 0.35E6));
                        fnew2 = 0.33 * ff;
```

```
                fprimenew2 = 0.67 * ff;
                fnew1 = 1.0 - (fnew2+fprimenew2);
                if (fnew1<0.0)
                {
                        fnew1=0.0;
                }
        }
        else if (fld > 1.0E6)
        {
                fnew2 = 0.33;
                fprimenew2 = 0.67;
        }
        phos[k].Lit = phos[k].nah * (B * Wx / TAU2) ;
        phos[k].actcharge = Nao-phos[k].nal-phos[k].nah;
        Prob3 = 3.14*radiu*radiu*(phos[k+1].Fn);
        R1 = Prob3*fnew1*phos[k].nal;
        R4 = phos[k].nah * (1.0/TAU2);
        phos[k].nt2 = (phos[k].nt2 > Nt2) ? Nt2 : phos[k].nt2;
        pt = Nt2-phos[k].nt2;
        R2A = Prob3*fnew2*fnew3;
        R2 = R2A * ((phos[k].nal <= pt) ? phos[k].nal : pt);
        R12A = Prob3*fprimenew2*fprimenew3;
        R12 = R12A * ((phos[k].nah <= pt) ? phos[k].nah : pt);
        sigma8 =  (fld > 400000.0) ? 0.0 : (1.0/(delta_Tdipole));
        R8 = sigma8 * ((phos[k].nt2 <= (Nao-phos[k].nal-phos[k].nah-
phos[k].condnband)) ?
                        phos[k].nt2 : (Nao-phos[k].nal-phos[k].nah-
phos[k].condnband));
        R3 = Prob3*fnew2*(1 - fnew3) * phos[k].nal;
        R13 = Prob3*fprimenew2*(1-fprimenew3)*phos[k].nah;

        /*

          if (((phos[k+1].Fn)/(fld*mobility)) > phos[k].actcharge)
          {
          R9 = ((phos[k+1].Fn)*sigma9)/(fld*mobility);
          }
          else
          {
          R9 = phos[k].actcharge*sigma9;
          }

        */
        R9 = 0.0;
        R5 = ((phos[k+1].Fn*(1.0/Wx)) > phos[k].actcharge*(1.0/delta_T)) ?
                (phos[k].actcharge)*(1.0/delta_T) : phos[k+1].Fn*(1.0/Wx);
```

```
                dnaldt = R4 - R1 - R2 - R3;
                dnahdt = R1 - R4 + R8 - R12 + R9 - R13 + R5;
                dnt2dt = R12 - R8 + R2;
                phos[k].Fn = phos[k+1].Fn + (R3 + R13 - R9 -R5)*Wx;
                dnt2 = dnt2dt * delta_T;
                phos[k].nt2 += dnt2;
                dnal = dnaldt * delta_T;
                phos[k].nal += dnal;
                dnah = dnahdt * delta_T;
                phos[k].nah += dnah;
                phos[k].condnband = (R3 + R13 - R9 - R5)*delta_T;
                total_charge = total_charge+(Nao-
(phos[k].nal+phos[k].nah+phos[k].nt2))*Wx;
        }
        if (flux_direction == 0)
        {
                flux_point = t_i;
        }
        flux_direction = 1;
        cathodic_interface();
    }

    void bulk_phosphor(void)
    {
        phos[n].Fn = 0.0;
        total_charge = nc1+nc11+na1+na11;
        if (phos[n].c3 < 0.0)
        {
                anodic_tunneling();
        }

        if (phos[0].Fn>phos[n].Fn)
        {
                forward_phosphor();
          }
        else
        {
                backward_phosphor();
        }

        return;
    }

    void anodic_tunneling(void)

    {
```

```
double fld1;
double Pa1,Pa11,d1,d11;
double f1,f11;

fld1 = phos[n].c3;

if(fld1>0.0)
{
        phos[n].Fn=0.0;
}
else
{
        register double cc; /* a temporary constant */

        fld1 = -fld1;
        cc = (-b2) / (fld1 * sqrt(m/m_star));
        d1 =  cc * pow(E1, 1.5);
        d11 = cc * pow(E11,1.5);
        cc =  a2 * pow( ( m/m_star), 0.125) * pow(fld1,0.25);
        Pa1 = cc * pow( E1, 0.625) * exp(d1);
        Pa11= cc * pow( E11, 0.625) * exp(d11);
        f1 = na1*Pa1;
        f11 = na11*Pa11;
        if(f1>na1/delta_T)
        {
                f1=na1/delta_T;
        }
        if(f11>na11/delta_T)
        {
                f11=na11/delta_T;
        }
        if(f1<0.0)
        {
                printf("f1<0 => Error in anodic interface \n");
                exit(0);
        }
        if(f11<0.0)
        {
                printf("f11<0 => Error in anodic interface \n");
                exit(0);
        }
        phos[n].Fn = f1 + f11;
        na1 = na1 - (f1*delta_T);
        if (na1<0.0)
        {
                f1 = f1+na1/delta_T;
```

```
                na1 = 0.0;
            }
            na11 = na11 - (f11*delta_T);
            if (na11<0.0)
            {
                f11 = f11+na11/delta_T;
                na11 = 0.0;
            }
    }

    return;
}


void cathodic_interface()
{
    register double dn1dt,dn11dt,dn1_11dt;

      dn1_11dt = nc1*Snd*Vth*(N11-nc11);
      dn1dt = phos[1].Fn-dn1_11dt;
    dn11dt=dn1_11dt;
      nc1 = nc1 + (dn1dt*delta_T);
      if (nc1<0.0)
      {
          nc1 = nc1 + (phos[1].Fn - dn1dt)*delta_T;
      }
      else
      {
          nc11 = nc11 + (dn11dt*delta_T);
      }
}

void anodic_interface()
{
    register double dn1dt,dn11dt,dn1_11dt;

      if (phos[n].Fn <0.0)
      {
          phos[n].Fn = - phos[n].Fn;
      }
    dn1_11dt = na1*Snd*Vth*(N11-na11);
    dn1dt = phos[n].Fn-dn1_11dt;
    dn11dt=dn1_11dt;
    na1 = na1 + (dn1dt*delta_T);
    if (na1<0.0)
      {
```

```
            na1 = na1 + (phos[n].Fn - dn1dt)*delta_T;
        }
        else
        {
            na11 = na11 + (dn11dt*delta_T);
        }
}

void exchange(void)  {
    int k;
    double temp1, temp11;

    for( k = 0; k < n/2; ++k ) {
        phos[k+1].nal = phos[n-k].nal;
        phos[k+1].nah = phos[n-k].nah;
        phos[k+1].nt2 = phos[n-k].nt2;
        phos[k+1].Fn  = phos[n-k].Fn=0.0;
    }

    phos[0].Fn = 0.0;

    temp1 = nc1;
    nc1 = na1;
    na1 = temp1;

    temp11 = nc11;
    nc11 = na11;
    na11 = temp11;

    return;
}

void constants(void) {
    register int k;
    register double A1,A2,A3,A4,A5,A6,A7;
    register double sum, sum1;
    register double activatorcharge;

    for( k=1; k<=n; ++k )          {
            activatorcharge = Nao-phos[k].nal-phos[k].nah;
            phos[k].spacecharge = activatorcharge - phos[k].nt2;
    }
    sum = 0.0;
    for( k=1; k<=n-1; ++k) {
            sum += phos[k].spacecharge;
    }
```

```
        /* WRD: some of these variables are never initialized!! */
        A1 = (q*W1*(1.0/ed)*(na1+/* na2+na3+na4+na5+na6+na7+na8+na9+na10+*/
na11-Neq));
        A2 = ((W1*ez/ed) + n*Wx) * (q/ez) * (nc1+ /*
nc2+nc3+nc4+nc5+nc6+nc7+nc8+nc9+nc10+*/ nc11-Neq) ;
        A3 = (q*Wx*W1/ed)*phos[n].spacecharge;
        A4 = ( (q*Wx*Wx)/(2.0*ez) ) * (sum + phos[n].spacecharge) ;
        A5 = ( (q*Wx)/ez ) * ( Wx + ((W1*ez)/ed) )  *  sum ;
        /*
        sum1 = 0.0;
        for( t=2; t<=(n-1); ++t) {
                sum2 = 0.0;
                for(k=1; k<=(t-1); ++k)
                        sum2 += phos[k].spacecharge;
                sum1 += sum2;
        }
        */
        /* WRD: this is equivalent to the above and is much faster */
        sum1 = 0.0;
        for(k=1 ; k <= n-2 ; ++k) {
                sum1 += (n - (k+1)) * phos[k].spacecharge;
        }

        A6 = (q*Wx*Wx) * (1.0/(ez)) * sum1 ;
        A7 = 2.0*W1 + ( ((n*Wx*ed)/ez) );
        c1 = ( Vapp + A1 + A2 - A3 - A4 - A5 - A6 ) * (1.0/ A7) ;
        phos[1].c3 = ( (ed * c1) - (q * (nc1 + /* nc2 +
                                                nc3+nc4+nc5+nc6+nc7+nc8+nc9+nc10+*/
nc11 - Neq) ) )
                * (1.0 / ez);
        for(k=1; k<=(n-1); ++k)   {
                phos[k+1].c3 = phos[k].c3 + (q*Wx/ez)*phos[k].spacecharge;
        }

        c5 = ( (ez*phos[n].c3) + (q*Wx* phos[n].spacecharge) - (q * (na1+ /*
na2+na3+na4+na5+na6+na7+na8+na9+na10+ */ na11-Neq)) ) * (1.0 / ed);

        return;
    }
```

```
/*************************************************************/
```

/***

Title: Constants.h

/***/

/* model parameters */

```
# define TAU2  100E-09 /* relaxation time */
# define radiu 4.999E-8 /* Radius for impact */
# define fnew3 0.6007 /* fraction impact ionized from lower energy level of the activator to the traps */
# define fprimenew3 0.6007 /* fraction impact ionized from higher energy level of the activator to the traps */
# define delta_Tdipole 5E-06 /* time for dipole collapse */
# define a1  9.0E+10
# define b1 1.49E+08
# define a2  9.0E+10
# define b2 1.49E+08
# define K 1 /* correction factor = k0.k1.k2.k3.k4 */
# define B 4.2E-19 /* luminance emitted in Joules for 1 transition from higher to the lower energy level of the activator */
# define sigma5 0.4E-3 /* fitting parameter for R5 */
# define sigma9 1E-3
# define delta1 1.0E-15
# define beta1 1.0E-17
# define beta2 1.0E-6
# define beta1p 2.53E-13
# define beta2p 2.53E-2
# define G1 1.0E-14
# define tau1 1.75E-6
# define delta_T1 1000E12
# define El1 3
# define delta_T 0.05E-06 /* simulation time interval */
# define Ts  9000 /* simulation duration */

/* applied voltage parameters */
# define Vs  123.0 /* applied voltage */
# define RISE_TIME 2000 /* rise time for the applied voltage pulse */
# define FALL_TIME 7000 /* fall time for the applied voltage pulse */
# define NO_OF_PULSES 200 /* total number of pulses */

/* phosphor parameters */
# define Nt2 1.00E19 /* density of traps */
# define Nao 1.00E19 /* density of activators */
```

```
# define Nc  3.14E+18 /* density of states in the conduction band */
# define ez 83.19E-14 /* dielectric constant of phosphor */
# define ed 69.92E-14 /* dielectric constant of insulator */
# define n 100 /* number of sections of phosphor */
# define Wz 0.513E-4 /* total width of the bulk phosphor layer */
# define Wx 0.513E-6 /* width of each of the 'n' sections of phosphor */
# define W1 1.525E-5 /* width of each insulator */

/*****************************************************************/

/* depth of interface states */
#define E1 0.4 /* depth of the shallowest interface state */
#define E2 0
#define E3 0
#define E4 0
#define E5 0
#define E6 0
#define E7 0
#define E8 0
#define E9 0
#define E10 0
#define E11 0.75533/* depth of the deepest interface state .7554 nothing */

/* density of interface states */
# define N1  5E+14 /* density of the shallowest interface state */
# define N2  0
# define N3  0
# define N4  0
# define N5  0
# define N6  0
# define N7  0
# define N8  0
# define N9  0
# define N10 0
# define  N11 10.0E+15 /* density of the deepest interface state */

/*****************************************************************/

/* physical constants */

# define m 9.1E-31
# define m_star 2.28E-31
# define mobility 100
```

```
# define SIGMA2   1.0E-8
# define SIGMA1  5.0E-11
# define SIGMA3 4.0E-5
# define Sn  1.0E-17
# define Snt  1.0E-16
#define  Vth  2.33E+07
# define Vsat 1.0E+07
# define Eb 1.06
# define Etc 0.4
# define KT 0.0259
# define ALPHA 2.0E-16
# define Neq  5.0E+15
# define Nto 0
# define q -1.6E-19
# define Snd 2.2E-17
```

```
/*****************************************************************/
```

Title: Variables.h

```
/*****************************************************************/
    FILE *Macrofile;
    FILE *FluxFile;
    FILE *Infofile;
    FILE *VILfile;
    FILE *EIfile;
    FILE *Scaledfile;
    FILE *Timefile;
    FILE *nahvsT;

    double e_cathode[100000], e_anode[100000];
    double max_e_cathode, max_e_anode, tot_luminance, totalflux;
    double fnew1;
    double nahct;
    double tot_lit;
    int flux_point;
    double flux_disp;
    double tot_flux_unscaled;
    double tot_flux_scaled;

    FILE *LvsT,*CvsT[n+1],*PatvsT,*PtcvsT,*D1vsT,*D5vsT,*DnvsT,*FvsT,
       *DvsT, *RhovsT,*FvsT,*F1vsT,*F5vsT,*FnvsT,*NtvsT,*NvsT, *V,
       *NSvsT, *Ro1vsT,*Ro5vsT,*RonvsT, *R8vsT, *Nt2vsT, *Nahvst, *Nahpt;
    /*These are all file-pointers*/


    FILE *Ex500vsT, *Rhox500vsT, *Ex1000vsT, *Rhox1000vsT, *Ex2000vsT,
       *Rhox2000vsT, *Ex3000vsT, *Rhox3000vsT,
       *Ex4000vsT, *Rhox4000vsT, *Ex4500vsT, *Rhox4500vsT; /* Electric Field as a
                                                              function of space */
    typedef struct phosphor_slice {
       double c3;
       double Fn;              /* Flux in each section of the phosphor region*/
                               /* Flux in cathode Fnc and Flux in Anode Fna */
       double nal, nah, nt2;
       double actcharge;
       double Lit;             /* Luminance in the ith. section at time t */
       double condnband;
       double spacecharge;     /* spacecharge = Nao-nal[i]-nah[i]-nt2[i] */
    } phosphor_t;
```

```
    phosphor_t phos[n+2];              /* most arrays only use up to n+1; Fn, JFn need up
to n+2 */

    double g;
    double pt, f3;
    double stfn;
    double chkfld;

    double chkvalue;
    double innerk;
    double max_flux_disp;
    double setr;
    int dum_count;
    double tot_charge;
    /*Prob. of tunneling(from:to)(a:activator,t:trap,c:conduction band)*/
    /* in (n+1)th. section */

    double total_charge;
    double dnt2;
    double fltot,fl1,fl2,fl3,fl4,fl5,fl6,fl7,fl8,fl9,fl10,fl11;
    double
    probb1,probb2,probb3,probb4,probb5,probb6,probb7,probb8,probb8,probb9,probb1
0,probb11;

    double dd1,dd2,dd3,dd4,dd5,dd6,dd7,dd8,dd9,dd10,dd11;
    double c1,c5,c6; /* constants */
    double nc1, /* nc2,nc3,nc4,nc5,nc6,nc7,nc8,nc9,nc10, */ nc11;
    double na1, /* na2,na3,na4,na5,na6,na7,na8,na9,na10, */ na11;
    double nca;
    double chrg;    /* nc11 = deepest interface state at cathode*/
    double Lt ; /* Luminance for the time slice */
    double funcu;
    /* int ctr_i; WRD: unused */
    long int j;
    long int t;
    double Lum[100000];
    double Vol[100000];
    double Flu[100000];
    long int run_t;
    double max_lum,max_v,max_flux;
    int t_i;
    int z;
    int flux_direction;
    double fld_tunnel;
    double lum_peak;
    /* To find the peak luminence of the positive pulses */
```

```
double L1, L2;          /*  To compare luminence peaks */

double Vapp;

double fnew2,fprimenew2,fnew1;
int set_tunnel;
‘*****************************************************************
```

VITA

Dharmashankar Rajagopalan was born in Kolkatta, West Bengal on December 22, 1980. He received his Bachelor's in Electrical and Electronics Engineering in 2002 from SRM College of Engineering, University of Madras in India. He worked as a Research Assistant from January 2003-December 2004 in the Department of Electrical and Computer Engineering. He is currently working as Test Engineer at SMC, Inc., Lexington, Kentucky.

_____

(Dharmashankar Rajagopalan)